2021

# Degradation of Benzyl Phenyl Ether as Lignin Model Compound by Electrochemical Advanced Oxidation Process in a Microreactor

Kevin Lee
*Faculty of Engineering*

# Degradation of Benzyl Phenyl Ether as Lignin Model Compound by Electrochemical Advanced Oxidation Process in a Microreactor

Mr. Kevin Lee



A Thesis Submitted in Partial Fulfillment of the Requirements
for the Degree of Master of Engineering in Chemical Engineering
Department of Chemical Engineering
FACULTY OF ENGINEERING
Chulalongkorn University
Academic Year 2021

การสลายตัวของเบนซิลฟีนิลอีเทอร์ซึ่งเป็นสารตัวแทนลิกนินด้วยการออกซิเดชันขั้นสูงเชิงไฟฟ้าเคมีในเครื่องปฏิกรณ์ขนาดไมโคร

นายเควิน ลี



วิทยานิพนธ์นี้เป็นส่วนหนึ่งของการศึกษาตามหลักสูตรปริญญาวิศวกรรมศาสตรมหาบัณฑิต
สาขาวิชาวิศวกรรมเคมี ภาควิชาวิศวกรรมเคมี
คณะวิศวกรรมศาสตร์ จุฬาลงกรณ์มหาวิทยาลัย
ปีการศึกษา 2564

| | |
|---|---|
| Thesis Title | Degradation of Benzyl Phenyl Ether as Lignin Model Compound by Electrochemical Advanced Oxidation Process in a Microreactor |
| By | Mr. Kevin Lee |
| Field of Study | Chemical Engineering |
| Thesis Advisor | Professor VARONG PAVARAJARN, Ph.D. |

Accepted by the FACULTY OF ENGINEERING, Chulalongkorn University in Partial Fulfillment of the Requirement for the Master of Engineering

..... Dean of the FACULTY OF ENGINEERING
(Professor SUPOT TEACHAVORASINSKUN, D.Eng.)

THESIS COMMITTEE

..... Chairman
(Assistant Professor PONGTORN CHAROENSUPPANIMIT, Ph.D.)

..... Thesis Advisor
(Professor VARONG PAVARAJARN, Ph.D.)

..... Examiner
(KRITCHART WONGWAILIKHIT, Ph.D.)

..... External Examiner
(Nawin Viriya-empikul, D.Eng.)

เควิน ลี : การสลายตัวของเบนซิลฟีนิลอีเทอร์ซึ่งเป็นสารตัวแทนลิกนินด้วยการออกซิเดชันขั้นสูงเชิงไฟฟ้าเคมีในเครื่องปฏิกรณ์ขนาดไมโคร. ( Degradation of Benzyl Phenyl Ether as Lignin Model Compound by Electrochemical Advanced Oxidation Process in a Microreactor) อ.ที่ปรึกษาหลัก : วรงค์ ปวราจารย์

-



| | | |
|---|---|---|
| สาขาวิชา | วิศวกรรมเคมี | ลายมือชื่อนิสิต ..... |
| ปีการศึกษา | 2564 | ลายมือชื่อ อ.ที่ปรึกษาหลัก ..... |

# # 6370035021 : MAJOR CHEMICAL ENGINEERING
KEYWORD: LIGNIN, ELECTROCHEMICAL ADVANCED OXIDATION PROCESS, DEGRADATION, MICROREACTOR, LIGNIN MODEL COMPOUND

Kevin Lee : Degradation of Benzyl Phenyl Ether as Lignin Model Compound by Electrochemical Advanced Oxidation Process in a Microreactor. Advisor: Prof. VARONG PAVARAJARN, Ph.D.

As the world is shifting away from its reliance on fossil fuel, lignocellulosic biomass, which is low cost, renewable and abundant with cellulose, hemicellulose and lignin being its major components. Lignin has high potential to be converted into other value-added chemicals as an alternative to fossil fuel. This research focusses on systematic investigation of degradation of lignin by electrochemical advanced oxidation process (EAOP) in a microreactor, using benzyl phenyl ether (BPE) as a model compound for lignin. The first part of the research investigates the dissolution of BPE in various volume fraction of co-solvent system. The co-solvent system is used because water is needed to generate hydroxyl radicals to cleave the α-O-4 bond between two aromatic rings in BPE via EAOP, while an organic solvent is used to dissolve BPE as it is insoluble in pure water. The effect of organic solvent volume fraction in the co-solvent system, in the range of 0% to 100%, on solubility of BPE was investigated, while the concentration of BPE was fixed at 100 mg/L. The results indicated that the solubility of BPE decreases as the volume fraction of organic solvent decreased. Volume fraction of 30% organic solvent in the co-solvent system is chosen as a balance between solubility and conversion. The second part of the research focusses on the degradation kinetics of BPE in the co-solvent system where the influence of mean residence time (27.0 - 81.0 s), applied current (0.93 - 8.33 $A/m^2$), concentration of solvent (30 - 50 vol% ethanol/water) and type of solvent (acetonitrile/water and ethanol/water). Intermediate products detected, partial pathways and partial mechanisms of the degradation of BPE are discussed at the final third section as well.



| | | |
|---|---|---|
| Field of Study: | Chemical Engineering | Student's Signature ..... |
| Academic Year: | 2021 | Advisor's Signature ..... |

# ACKNOWLEDGEMENTS

This project is possible thanks to the guidance and assistance from many different parties. First and foremost, I would like to express my appreciation to Chulalongkorn University for providing this opportunity to me to complete my Master's Degree Thesis.

I would like to acknowledge and appreciate my thesis advisor, Professor Varong Pavarajarn for the guidance and help when I faced any problems or hardship when I am completing my thesis. His guidance and assistance help me pull through the endless problems given to me while completing my thesis. Furthermore, I would also like to take the time to thank the people in Excellence in Particle and Technology Engineering Laboratory, Chulalongkorn University for providing the resources and assistance for the whole period of my studies.

Lastly, I would also like to thank my family, girlfriend and friends for the endless support and encouragement given to me while finishing my thesis during this time of great struggle.

Kevin Lee

# TABLE OF CONTENTS

**Page**

# LIST OF FIGURES

# LIST OF TABLES

# CHAPTER 1

# INTRODUCTION

## 1.1 Background Studies

The usage of fossil fuels are the most dominant resources in the global energy production and chemical productions for industrial applications with more than 80% originate from either crude oil, natural gas or coal [1]. Figure 1.1 shows that the global fossil fuel consumption increased exponentially since the 1950s [2]. Even though the emission growth has slowed down recently but it is already at the peak producing 135,000 TWh annually. The main contributing factor is surge of human population and demand which increases the demand of fossil fuels leading to the higher global carbon emissions. The increase in emission can have drastically change the quality of life and climate regionally and globally [3]. Therefore, there is a global demand for the development of new methods for the production of alternative fuels from renewable and sustainable sources to lower reliance on fossil fuel.

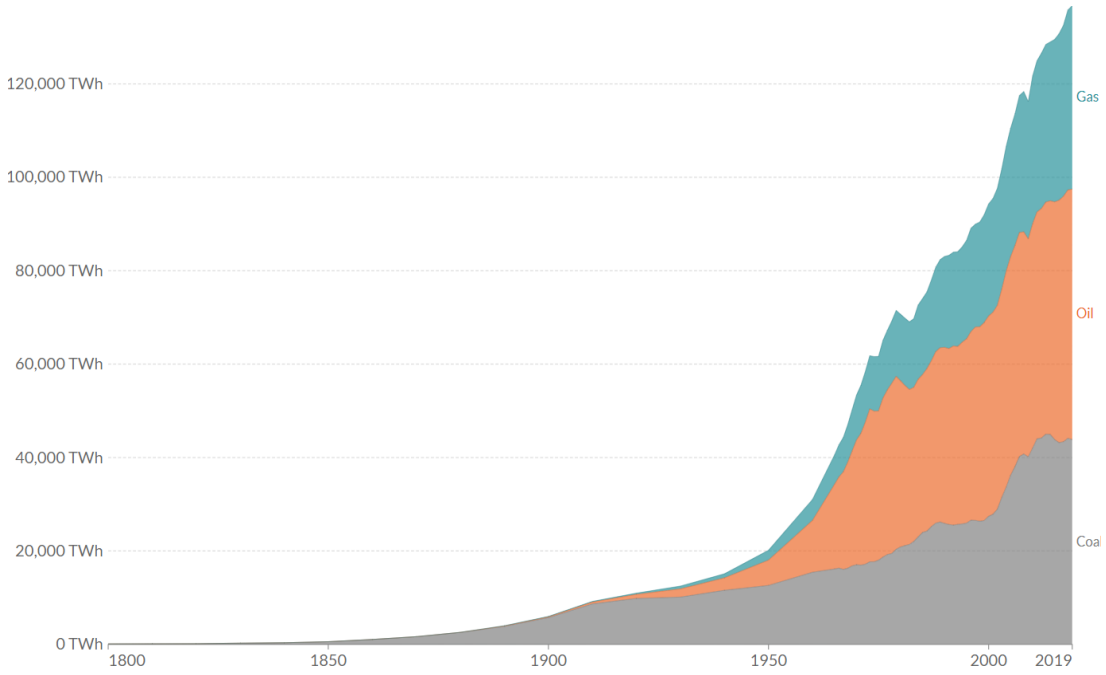


Figure 1.1 Global fossil fuel consumption data from 1800 to 2019 [2]

As one of the most widely available biomass, lignocellulosic (LC) biomass which is low cost, renewable and abundant with cellulose, hemicellulose and lignin being its major components has a high potential to be converted into other value-added chemicals such as biofuels, bioplastics and biofertilizers or precursors for polymer synthesis [4], [5]. Lignin is an amorphous three-dimensional polymer being interconnected or cross-linked by chemical bonds such as carbon-carbon (C-C) bond and ether (α-O-4, β-O-4) bond. Lignin being formed in nature has been estimated to be ranging from 0.5 to 3.6 billion tons annually as well as the production of lignin annually at around 40 to 60 million tons from paper and pulp industry and 100,000 to 200,000 tons from cellulosic ethanol industry mainly as a by-product [5]–[8]. Lignin being abundant, aromatic and highly functionalized has the potential for being a renewable and sustainable raw material for the production of value-added chemicals [9]. Furthermore, utilization of lignocellulosic biomass is environmentally friendly due to the lower emissions of nitrogen oxides (nox) sulfur dioxide (SO2) and no net emission of carbon dioxide (CO2) [10]–[12]. Overall, the utilization of biomass can lead towards a carbon neutral future by generating lower emissions compared to fossil fuels [12].

Utilization of lignin as raw material for green production of value-added compounds requires depolymerization of lignin. Depolymerization of lignin can be done by various physiochemical approaches such as pyrolysis, gasification, hydrogenolysis and oxidation but these methods require stringent conditions and high energy input to achieve the high temperature and/or high pressure required which often results to serious obstacles to achieve a practical, cost-effective process [13]. In this work, electrochemical advance oxidation (EAOP), which is a technique relying on oxidation by hydroxyl radicals electrochemically generated from water, is used for depolymerization at room temperature. Nevertheless, due to the complexity of the lignin structure, this research focuses on the degradation of benzyl phenyl ether (BPE) as the lignin model compounds. A co-solvent system is used because water is needed to generate hydroxyl radicals to cleave the α-O-4 bond between two aromatic rings in BPE via EAOP while another solvent is used to dissolve BPE as it is insoluble in pure water. Microreactor was used to eliminate mass transfer resistance within the reactor so that true kinetics could be investigated. However, to date, no other research accessed the degradation of lignin or lignin model compounds using hydroxyl radicals generated through EAOP in a co-solvent system.



## 1.2 Objectives

The objective of this research is to study the degradation performance of benzyl phenyl ether as lignin model compound in a co-solvent system through electrochemical advanced oxidation process (EAOP) in a microreactor where the kinetics, intermediate products detected, partial pathways and partial mechanisms of the degradation are determined.

## 1.3 Structure of thesis

The thesis consists of 5 main chapters as shown below:

Chapter I proposes the motivation and introduction of this research.

Chapter II explains the theory and literature reviews related to lignin and degradation of lignin.

Chapter III mentions about the chemicals and equipment used, experiment setup and analytical method.

Chapter IV discusses about the results of gained from this research.

Chapter V summarizes the results and give recommendations.

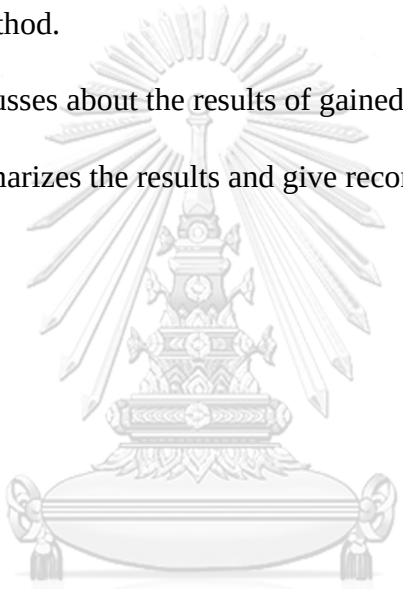

# CHAPTER 2

# LITERATURE REVIEW

## 2.1 Background

### 2.1.1 Lignocellulosic biomass and lignin

Lignocellulosic biomass is a complex architecture consisting of 40%-50% cellulose, 25%-30% hemicellulose and 10%-30% lignin as the three major biopolymer components. Figure 2.1 illustrates the lignocellulosic biomass main components with lignin itself composing of three main phenolic components which are p-coumaryl alcohol, coniferyl alcohol and sinapyl alcohol [14]. Lignin which enables the plant to grow high by providing stiffness to the plant are formed when the plant undergoes lignification. Lignin can be synthesized by the polymerization of the three phenolic components with the ratio varying depending on the types of plants.

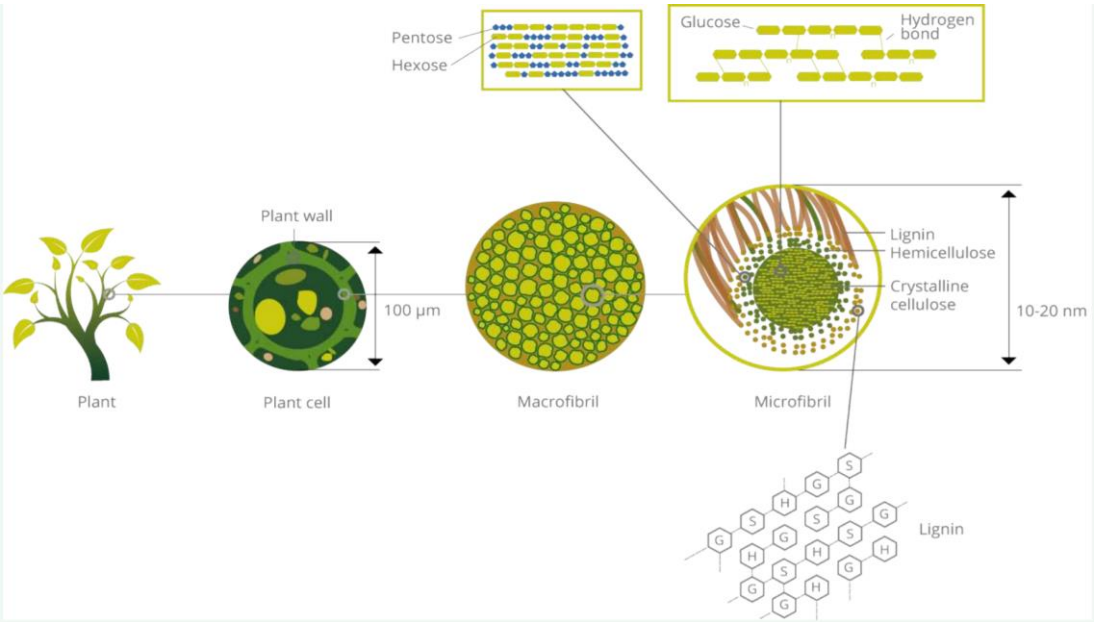


Figure 2.1 Illustration diagram of lignocellulose with the hexagons representing the lignin units, p-coumaryl alcohol (H), coniferyl alcohol (G) and sinapyl alcohol (S) [14]

#### 2.1.1.1 Lignocellulosic composition

The percentage ratio of cellulose, hemicellulose and lignin present depends on the type of plants as different plants affects the ratio as shown in Figure 2.2. Therefore, the contents can go as low as 0 wt% in cotton and all the way up to 40 wt% for nut shells [15].

| Feedstocks | Carbohydrate composition (% dry wt) | | |
|---|---|---|---|
| | Cellulose | Hemicellulose | Lignin |
| Barley hull | 34 | 36 | 19 |
| Barley straw | 36–43 | 24–33 | 6.3–9.8 |
| Bamboo | 49–50 | 18–20 | 23 |
| Banana waste | 13 | 15 | 14 |
| Corn cob | 32.3–45.6 | 39.8 | 6.7–13.9 |
| Corn stover | 35.1–39.5 | 20.7–24.6 | 11.0–19.1 |
| Cotton | 85–95 | 5–15 | 0 |
| Cotton stalk | 31 | 11 | 30 |
| Coffee pulp | 33.7–36.9 | 44.2–47.5 | 15.6–19.1 |
| Douglas fir | 35–48 | 20–22 | 15–21 |
| Eucalyptus | 45–51 | 11–18 | 29 |
| Hardwood stems | 40–55 | 24–40 | 18–25 |
| Rice straw | 29.2–34.7 | 23–25.9 | 17–19 |
| Rice husk | 28.7–35.6 | 11.96–29.3 | 15.4–20 |
| Wheat straw | 35–39 | 22–30 | 12–16 |
| Wheat bran | 10.5–14.8 | 35.5–39.2 | 8.3–12.5 |
| Grasses | 25–40 | 25–50 | 10–30 |
| Newspaper | 40–55 | 24–39 | 18–30 |
| Sugarcane bagasse | 25–45 | 28–32 | 15–25 |
| Sugarcane tops | 35 | 32 | 14 |
| Pine | 42–49 | 13–25 | 23–29 |
| Poplar wood | 45–51 | 25–28 | 10–21 |
| Olive tree biomass | 25.2 | 15.8 | 19.1 |
| Jute fibres | 45–53 | 18–21 | 21–26 |
| Switchgrass | 35–40 | 25–30 | 15–20 |
| Grasses | 25–40 | 25–50 | 10–30 |
| Winter rye | 29–30 | 22–26 | 16.1 |
| Oilseed rape | 27.3 | 20.5 | 14.2 |
| Softwood stem | 45–50 | 24–40 | 18–25 |
| Oat straw | 31–35 | 20–26 | 10–15 |
| Nut shells | 25–30 | 22–28 | 30–40 |
| Sorghum straw | 32–35 | 24–27 | 15–21 |
| Tamarind kernel powder | 10–15 | 55–65 | – |
| Water hyacinth | 18.2–22.1 | 48.7–50.1 | 3.5–5.4 |



Figure 2.2 Composition of cellulose, hemicellulose and lignin in different plants [15]

### 2.1.1.2 Lignin chemical structure

The chemical structure of lignin monolignols precursors including p-coumaryl alcohol (H), coniferyl alcohol (G) and sinapyl alcohol (S) are as shown in Figure 2.3. The composition of the monolignols in lignin depends on the type of plant species. Typically, dicotyledonous angiosperm also known as hardwood lignin consist of mainly G and S units with traces of H units while gymnosperm also known as softwood lignin consist of mainly G units and low amount of H units. Meanwhile,

lignin from grasses (monocots) have almost equal amount of G and S units with more H units than dicots [16].

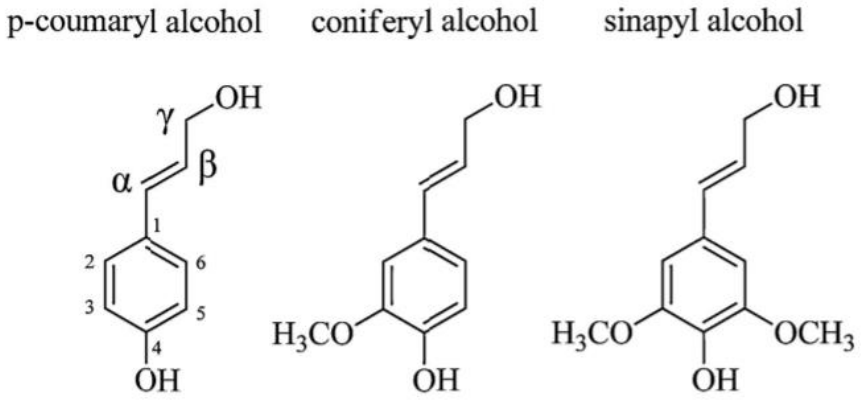


Figure 2.3 Three monolignols precursors present in the lignin chemical structure [17]

The three monolignols are linked together during the biological lignification process carried out by plants either by carbon-carbon bond or ether with two-thirds or more of the linkages being ether while the others are carbon-carbon bonds. In order to differentiate various linkages present between two of the lignin monolignols, Greek letters α, β, and γ are used to number the propyl carbon chain next to the benzene ring while the carbon atoms present inside the benzene ring are numbered 1 to 6 as shown in Figure 2.3 [18]. Using β-O-4 as an example, β-O-4 linkage can be understood as the β carbon atom on the propyl carbon chain connected to an oxygen atom at the 4$^{th}$ position on another benzene ring. The common linkages between the monolignols include β-O-4 (β-aryl ether), β−β (resinol) and β-5 (phenylcoumaran) while other linkages include α-O-4 (α-aryl ether), 4-O-5 (diaryl ether), 5−5, α-O-γ (aliphatic ether) and β-1 (spirodienone). [19] The illustration of the linkages is as shown in Figure 2.4 of a softwood lignin while the percentage of such linkages are compiled in Table 2.1. The percentages of each linkage are determined by the contribution of each monolignols during the polymerization process. As shown in Table 2.1, β-O-4 (β-aryl ether) linkage has the highest percentage at as high as 50% for softwood and 65% for hardwood [19].

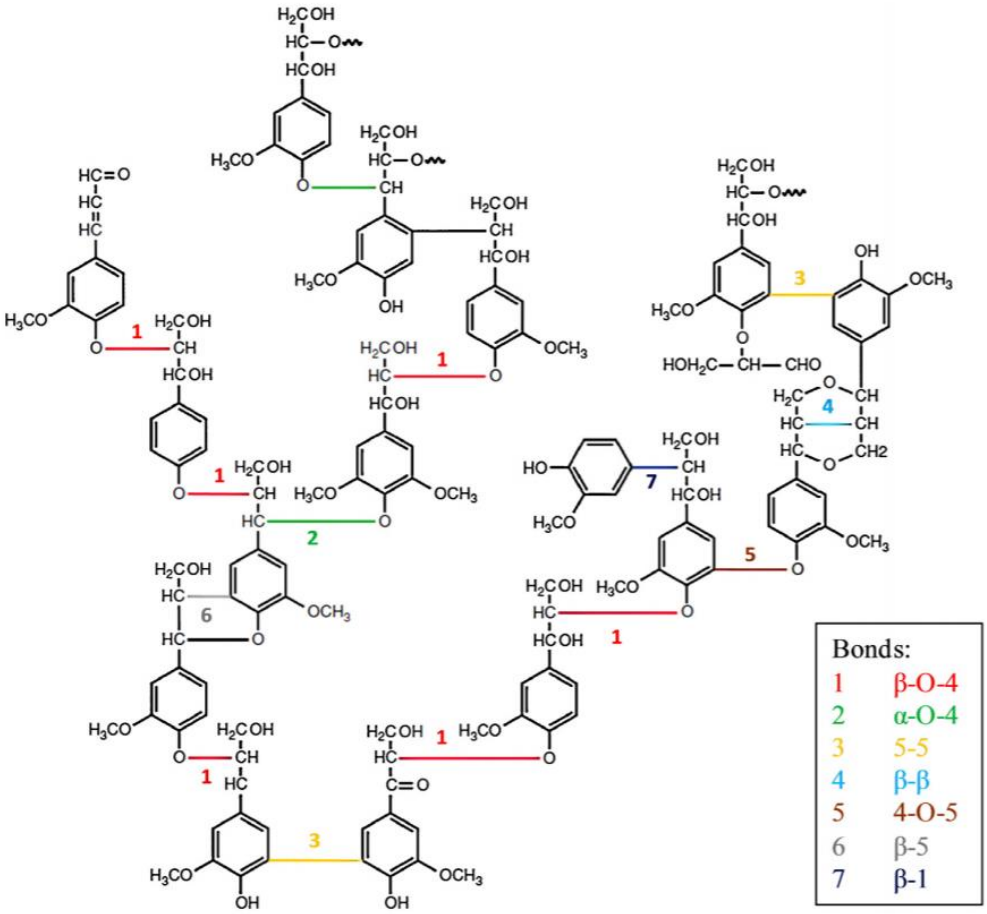


Figure 2.4 The main linkages in softwood lignin [17]

Table 2.1 Frequency of lignin linkages in both softwood and hardwood [19]

| Linkages | Linkages (%) | |
|---|---|---|
| | Softwood | Hardwood |
| β-O-4 | 43-50 | 50-65 |
| β-5 | 9-12 | 4-6 |
| α-O-4 | 6-8 | 4-8 |
| β- β | 2-4 | 3-7 |
| 5-5 | 10-25 | 4-10 |
| 4-O-5 | 4 | 6-7 |
| β-1 | 3-7 | 5-7 |
| Others | 16 | 7-8 |

### 2.1.2 Lignin extraction processes and resulting products

Lignin is one of the components including cellulose and hemicellulose making up lignocellulosic biomass. Lignin is extracted from the lignocellulosic by means of physical, chemical or biochemical treatments or even a combination of a few different treatments. The extraction processes and conditions from pulping or delignification can greatly affect the structure of the lignin product, purity and properties [20]. The pulping processes are based on the breaking or cleaving the ester and ether bondage [17]. Figure 2.5 shows the commercial processes that are used to separate lignin with the extraction process having two main categories which are sulfur or sulfur-free processes. Table 2.2 shows the properties of the differeent technical lignins.

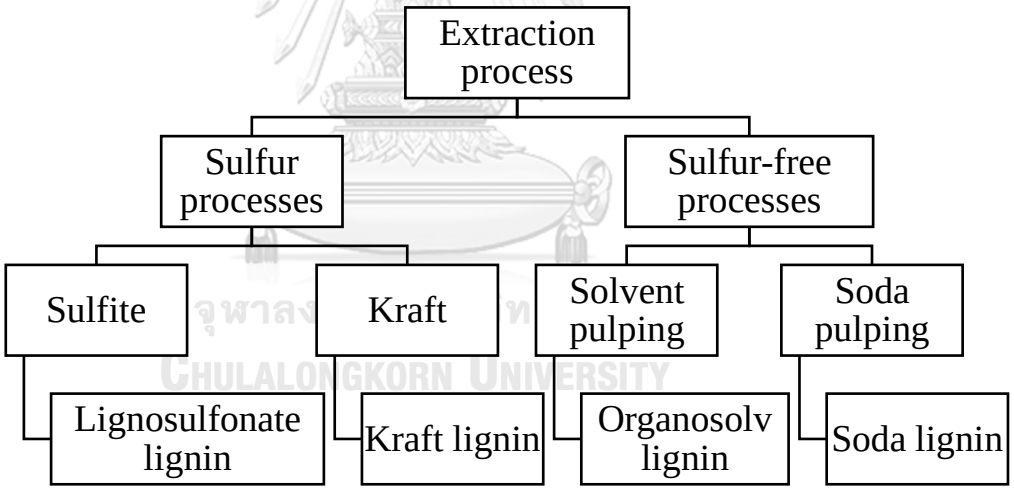


Figure 2.5 Processes that separates lignin from lignocellulosic biomass with the resulting lignin [17]

Table 2.2 Properties of technical lignins [17]

| Lignin Type | Sulfur-lignins | | Sulfur-free lignins | |
|---|---|---|---|---|
| | Kraft | Lignosulfonate | Soda | Organosolv |
| Raw materials | Softwood<br>Hardwood | Softwood<br>Hardwood | Annual plants | Softwood<br>Hardwood<br>Annual plants |
| Solubility | Alkali<br>Organic solvents | Water | Alkali | Wide range of organic solvents |
| Polydispersity | 2.5-3.5 | 6-8 | 2.5-3.5 | 1.5-2.5 |
| Average molar mass (g $mol^{-1}$) | 1000-3000 | 15000-50000 | 800-3000 | 500-5000 |
| $T_g$ (°C) | 140-150 | 130 | 140 | 90-110 |

#### 2.1.2.1 Sulfur lignins

The sulfur lignins are mainly produced from the pulp and paper industries including kraft lignin and lignosulfonate lignin which are extracted from the cellulose. The kraft lignin going through the kraft process uses both chemicals which are sodium hydroxide (NaOH) and sodium sulfide ($Na_2S$) whereas lignosulfonate lignin through the sulfite process of cooking aqueous sulfur dioxide ($SO_2$) and a base with examples including magnesium and sodium. The black liquid generated from both processes are acidified to recover the lignin [17]. Kraft lignin are extracted in high sulfur environment but the sulfur content in the residual is low at around 1% to 2%. Besides, it also contains condensed structures and phenolic hydroxyl groups at a high amount due to the cleaving of the β-aryl bonds at the cooking process. The average molar mass of kraft lignin is 1000 to 3000 g $mol^{-1}$ [21]. In contrast, lignosulfonate lignin contains higher amount of sulfur in the sulfonate groups form. Lignosulfonate lignin are also water soluble with a higher molar mass compared to other lignins and polydispersity of 6 to 8 [22]. Due to these properties, lignosulfonate lignin is highly

used in some industrial applications producing products such as binders, surfactant, adhesives and dispersing agent.

#### 2.1.2.2 Sulfur-free lignins

The sulfur-free lignins including soda lignin from alkaline pulping and organosolv lignin from solvent pulping is a new lignin product that came out which have low macromolecular size after the fraction steps. The structure of these lignins show resemblance to the structure of native lignins. Moreover, these lignins have properties that can potentially turn them into a source of low-molar mass phenol or aromatic compounds [17]. Organosolv lignin has the highest quality and purity among the other lignins [23]. Moreover, organosolv lignin due to its hydrophobicity are not soluble in water but soluble in most organic solvent. The common organosolv lignin extraction process involves the use of ethanol water pulping as well as pulping with acetic acid with mineral acid such as sulfuric and hydrochloric acid present. On the other hand, soda lignin based cooking methods are mainly obtained from annual plants like bagasse, flax and straw. Soda lignin extraction is based on hydrolytic cleavage of the native lignin but leads to a resulting product lignin that is chemically unmodified compared to other lignins. Soda lignin potentially have high silicate and nitrogen due to the process of extraction [17].

### 2.1.3 Lignin model compounds

Lignin that are naturally polymerized consist of huge network of highly functionalized alkyl aryl ether monomers that are linked together by different linkages such as β-O-4 linkage (43 to 65% of all linkages). Lignin can potentially be converted into high value-added chemicals or precursors for polymer synthesis by breaking such

linkages which enables lignin to be a potential alternative to fossil fuels [24]. However due to the complexity of lignin with its many different linkages, it poses a significant challenge during analysis which is further caused by the high molecular weight of lignin. Therefore, lignin model compounds have been used to overcome these challenges with the objective of studying the structure and reactivity of lignin with some of the examples shown in Table 2.3 [18]. Lignin model compounds uses a simpler compound compared to lignin that typically mimic one of the linkages in lignin for example 2-phenoxyacetophenone was used to study the β-O-4 linkage.

Table 2.3 Examples of compounds being used as lignin model compounds

| Compound name | CAS NO. | Molecular Structure | Linkages | Reference |
|---|---|---|---|---|
| 2-phenoxyacetophenone | 721-04-0 | 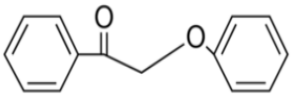 | β-O-4 | [24] |
| Benzyl phenyl ether | 946-80-5 | 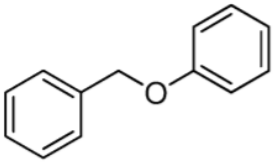 | α-O-4 | [9], [25] |
| Diphenyl ether | 101-84-8 | 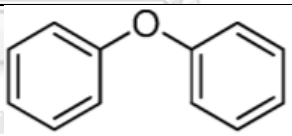 | 4-O-5 | [25] |
| Diphenyl methane | 101-81-5 | 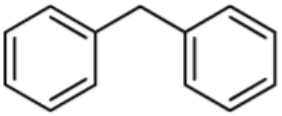 | β-1 | [25] |
| Biphenyl | 92-52-4 | 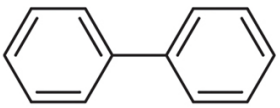 | 5-5 | [25] |

#### 2.1.3.1 Application of lignin model compounds

Lignin model compounds are used primarily to focus on the structure and reactivity of lignin from a perspective that is not achievable from using lignin due to the complexity and high molecular weight. The benefits and limitations of using lignin model compounds over lignin itself are summarized in Table 2.4:

Table 2.4 Benefits and limitations of using lignin model compounds over lignin [18]

| Benefits of using lignin model compounds | Limitations of using lignin model compounds |
|---|---|
| 1. Simplification of product stream from depolymerization for analysis.<br>2. Able to study the reaction mechanism in detail at different complexity.<br>3. Only one or a combination of few linkages can be chosen for analysis.<br>4. Confirmation of the formation of new motifs in lignin. | 1. Absence of the full version of lignin in terms of variation and complexity.<br>2. Additional impurities present.<br>3. Different solubility constraints.<br>4. Cannot replicate the 3D environment of lignin.<br>5. Cannot replicate complex product stream to create possible separation pathway. |



### 2.1.4 Electrochemical Advanced Oxidation Process (EAOP)

Electrochemical Advanced Oxidation Processes (EAOPs) have been developed from the conventional Advanced Oxidation Processes (AOPs) mainly for the treatment of wastewater stream to prevent environmental pollution. Due to industrial waste being very diverse containing both mixture of organic and inorganic compounds, no universal waste treatment is available so it depends on the nature and concentration of the pollutants measured in chemical oxygen demand (COD) shown

in Figure 2.6. Biological treatments are applied in waste that are polluted with organic compounds as it is the cheapest process but toxic or biorefractory molecules may hinder this process whereas traditional incineration process is used in high concentration waste but causes emission problems and not easily controlled. Meanwhile, chemical oxidation uses chlorine, ozone or hydrogen peroxide to treat contaminants that are biorefractory or reduce it to safe or biodegradable products, but some intermediate products may remain that are similar or even higher in toxicity than the initial compounds. In these situations, AOPs as a special class of oxidation technique can be used to remove these pollutants [26].

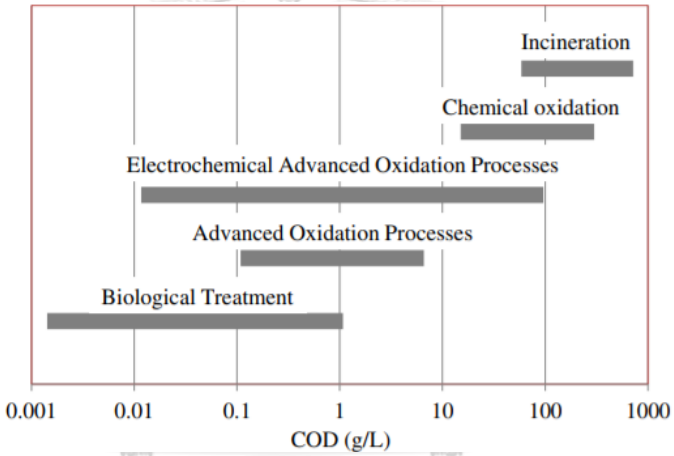


Figure 2.6 Applicability of waste treatment technologies according to the chemical oxygen demand [27]

Advanced Oxidation Processes (AOPs) can be defined as aqueous phase oxidation methods based on the intermediacy of highly reactive species in the mechanisms leading to the breaking down of the target pollutant. The hydroxyl radical ($OH^*$) shown in Figure 2.7, is a strong oxidant that can destroy most organic or organometallic contaminants till complete mineralization turning it into carbon dioxide, water or inorganic ions. Recently, new AOPs based on electrochemical knowledge have created Electrochemical Advanced Oxidation Processes (EAOPs) [26]. AOPs require chemical or other methods (UV or catalysis) to generate radicals which usually leads to harsh conditions and worse for the environment whereas

EAOPs overcome this by generating electrons through electrochemistry meaning the oxidation process is driven by electricity rather than chemicals to produce radicals [28]. The $OH^*$ are formed through equation (2.1) through oxidation on the anode surface. However, due to the $OH^*$ being reactive, it's rarely found in the reaction media as it reacts with other components through equation (2.2) and (2.3). The compounds that $OH^*$ can react with is the targeted compound as well through equation (*2.4*) mineralizing the targeted compound [29]. The advantages provided from EAOPs are highly efficient, amenability to automation, safety, easy handling and versality because it can handle effluents with COD level from 0.01 to 100 g/L. However, the disadvantages of it are electricity cost, low conductance wastewater require electrolytes addition, loss of activity and shortening of electrode lifespan by fouling due to the deposition of organic material on the electrode surface. The factors that affect the efficiency of EAOPs include the applied current, type of electrodes combination, temperature, electrolyte and pH of solution [26].

| Oxidizing agent | Standard potential (V vs. SHE) |
|---|---|
| Oxygen (molecular) | 1.23 |
| Chlorine dioxide | 1.27 |
| Chlorine | 1.36 |
| Ozone | 2.08 |
| Oxygen (atomic) | 2.42 |
| Hydroxyl-radical | 2.80 |
| Fluorine | 3.06 |
| Positively charged hole on $TiO_2$ | 3.2 |

Figure 2.7 Standard potential of some oxidizing species

$$H_2O \rightarrow OH^* + H^+ + e^- \quad (2.1)$$

$$OH^* + OH^* \rightarrow H_2O_2 \quad (2.2)$$

$$H_2O_2 + OH^* \rightarrow H_2O + HO_2^* + H_2O \quad (2.3)$$

$$\text{Compound} + OH^* \rightarrow \text{Compound minerization products} \quad (2.4)$$

## 2.2 Literature survey

### 2.2.1 Degradation of benzyl phenyl ether α-O-4 lignin model compounds

This section discusses about the various factors that effects the degradation of α-O-4 lignin model compounds using benzyl phenyl ether as the compound in a co-solvent system. The various factors include the effects of the types of co-solvent systems and co-solvent ratio.

#### 2.2.1.1 Effect of types of solvents and ratio

The selection of a good solvent is important to ensure that the reactant which in this case is benzyl phenyl ether (BPE) to fully dissolve in the solution. According to the chemical data sheet sources, BPE is insoluble in water but soluble in most organic solvents [30]. However, water is crucial in providing free radicals for the electrochemical reaction to occur so a co-solvent system consisting of an organic solvent and water are used. Matsagar et al. (2018) carried out a study using various types of co-solvent systems (organic/water; 3/7 (v/v)) and pure solvents to investigate the conversion of BPE by hydrogenolysis. The pure solvents used were $H_2O$, MeOH, 2-Butanol, 1-Butanol, 2-Propanol, DMA, THF and EtOH shown in Figure 2.8 while the co-solvents used were 2-Butanol/$H_2O$, 2-Propanol/$H_2O$, DMA/$H_2O$, THF/$H_2O$, MeOH/$H_2O$ and EtOH/$H_2O$ shown in Figure 2.9. Comparing the pure and co-solvents in Figure 2.8 and Figure 2.9, the use of pure solvents show the highest conversion at 54% using pure $H_2O$ while co-solvents show the highest conversion at 91% using EtOH/$H_2O$ shows that a mixture of an organic solvent and $H_2O$ have higher conversion than pure solvents [12].

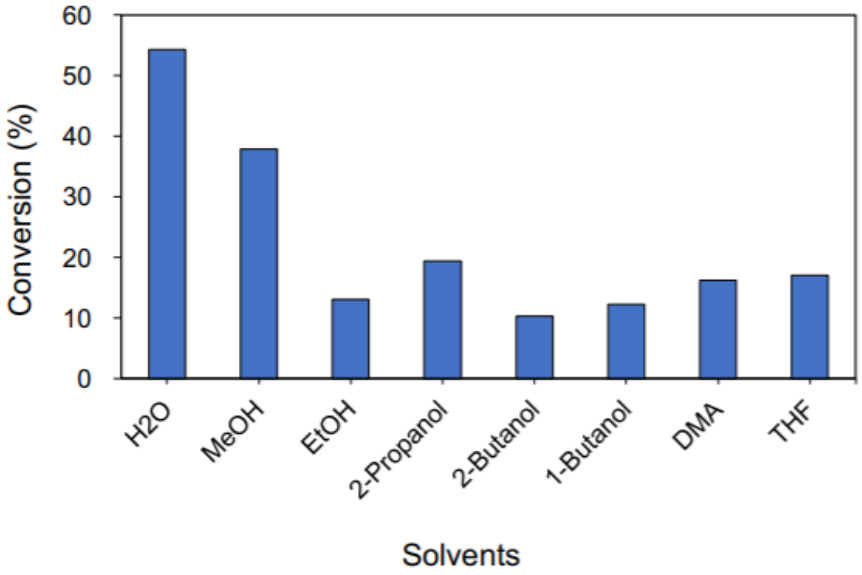


Figure 2.8 Effect of various types of pure solvents on BPE conversion. Reaction condition: BPE 0.0368 g, NaBH4 0.05 g, Ni/CB 0.04 g, solvent 10 mL, 70 °C, 1h [12]

Moreover, comparing the co-solvents in Figure 2.9, MeOH/$H_2O$ and EtOH/$H_2O$ shows the highest BPE conversion at 83% and 91% [12]. However, the solubility of BPE in MeOH/$H_2O$ is poor compared to in EtOH/$H_2O$ according to Grojzdek et al. (2020) [9]. Therefore, EtOH/$H_2O$ is the preferred co-solvent system for the conversion of BPE.



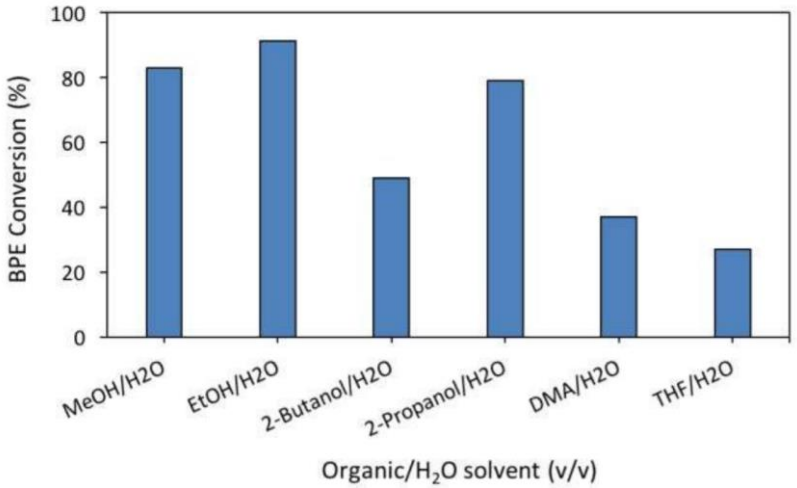


Figure 2.9 Effect of various types of co-solvents on BPE conversion. [12]

### 2.2.1.2 Effect of co-solvents ratio

The ratio of the co-solvents also effects the solubility and conversion of BPE in the solution. Matsagar et al. (2018) carried out a study the effect of EtOH/H2O co-solvent ratio on the conversion of BPE as shown in Figure 2.10. The solubility increases as the volume fraction of EtOH increases but the conversion decreases. As the volume fraction of EtOH increases from 0% to 30%, the conversion of BPE increased from 1.8% to 62%. Unfortunately, further increase in the EtOH volume fraction to 100% can improve the solubility of BPE to 100% but the conversion drops to 13% [12].

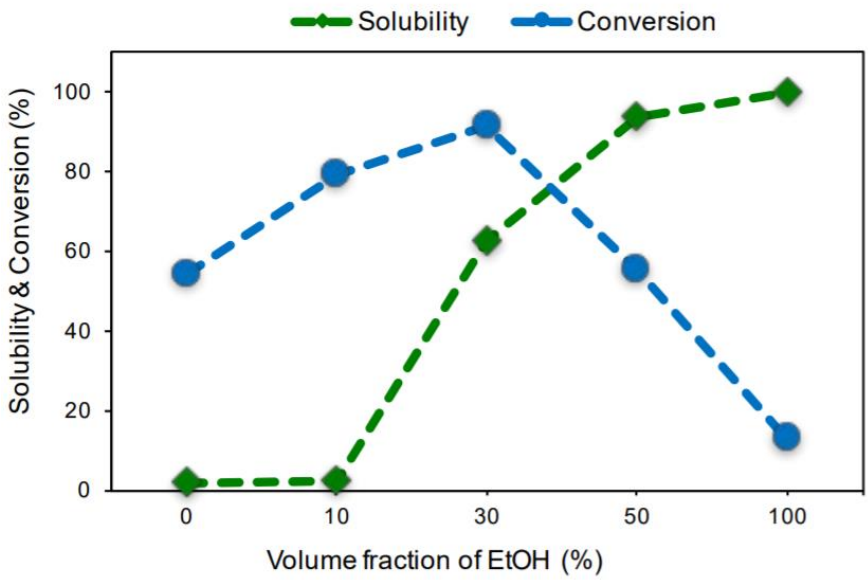


Figure 2.10 Solubility of BPE and its conversion in different volume fractions of EtOH in $H_2O$-EtOH co-solvent system.[12]

### 2.2.2 Summary of literature survey

Through literature survey, there are some past research that have been conducted to investigate the degradation of BPE in co-solvent system such as in ethanol/water and methanol/water via methods such as hydrogenolysis and acidolysis. These methods are often conducted in hash conditions requiring high temperature and/or high pressure which requires high input of energy leading to barriers to achieve a cost-effective process. To date, no other research accessed the degradation of BPE as α-O-4 lignin model compound in normal room conditions such as using hydroxyl radicals generated through EAOP in a microreactor. In this research, the potential of utilizing EAOP in a microreactor in normal room conditions to degrade BPE is investigated.

# CHAPTER 3

# METHODOLOGY

## 3.1 Study design

This section presents the list of materials and equipment used and experiment setup to achieve the objectives of the project.

### 3.1.1 List of material used

All reactants, gases, solvents and external calibration standard were of reagent grade and used as purchased without further purification with the specific specifications as follows: benzyl phenyl ether (BPE, 98% purity, Sigma Aldrich, St. Louis, MO, USA, CAS number 946-80-5), ethyl alcohol (EtOH, 99.9% purity, AR grade, Quality Reagent Chemical, QREC, New Zealand), acetonitrile (MeCN, 99.9% purity, HPLC grade, Quality Reagent Chemical, QREC, New Zealand), potassium iodide (KI, 99.0% purity, AR grade, KEMAUS, Cherrybrook, NSW, Australia), sodium hydroxide (NaOH, 97.0% purity, AR grade, KEMAUS, Cherrybrook, NSW, Australia), potassium hydrogen phthalate ($C_8H_5KO_4$, 99.5% purity, AR grade, Loba Chemie, Colaba, Mumbai, India), ammonium molybdate tetrahydrate ($(NH_4)6Mo7O_{24}.4H_2O$, 99.3% purity, AR/ACS grade, Loba Chemie, Colaba, Mumbai, India) and deuterium oxide ($D_2O$, 99.96% purity, Euristop, Gif-surYvette, France).

### 3.1.2 List of equipment

The apparatus or equipment that is required in this project for the electrochemical advanced oxidation in a microreactor includes:

1. Microreactor
2. Syringe pump
3. Dc power supply
4. Basic laboratory glass wares
5. Connecting wires
6. Multimeter
7. Weighing scale
8. Spatula

As for the characterization, the equipment needed are as follows:

1. Ultraviolet–Visible spectroscopy (UV-Vis)
2. Gas Chromatography–Mass Spectrometry (GCMS)
3. Gas Chromatography-Flame Ionization Detector (GC-FID)
4. Nuclear Magnetic Resonance spectrometer (NMR)

### 3.1.3 Reactor setup

The reactor used in this research is a microreactor. The microreactor used for this work is a microchannel with a width of 10 mm and length of 27 mm. The microchannel was created using a Teflon sheet with a cutout opening placed in between two electrodes. The height or thickness of the microreactor is determined by

the thickness of the Teflon sheet which was fixed at 250 µm. The layout of the reactor is as shown in Figure 3.1 while the components as well as the side and front view of the reactor are as shown in Figure 3.3. The surface area of the microreactor is 10mm x 27mm with the Teflon sheet thickness at 250 micrometers. The anode was soaked in the solution containing BPE for 24 hours prior to the reactor assembly to ensure complete adsorption of BPE on the graphite sheet during the experiment. The reactants enter through the bottom of the reactor which will come in contact with the anode and cathode then leaves the reactor at the side of the reactor.

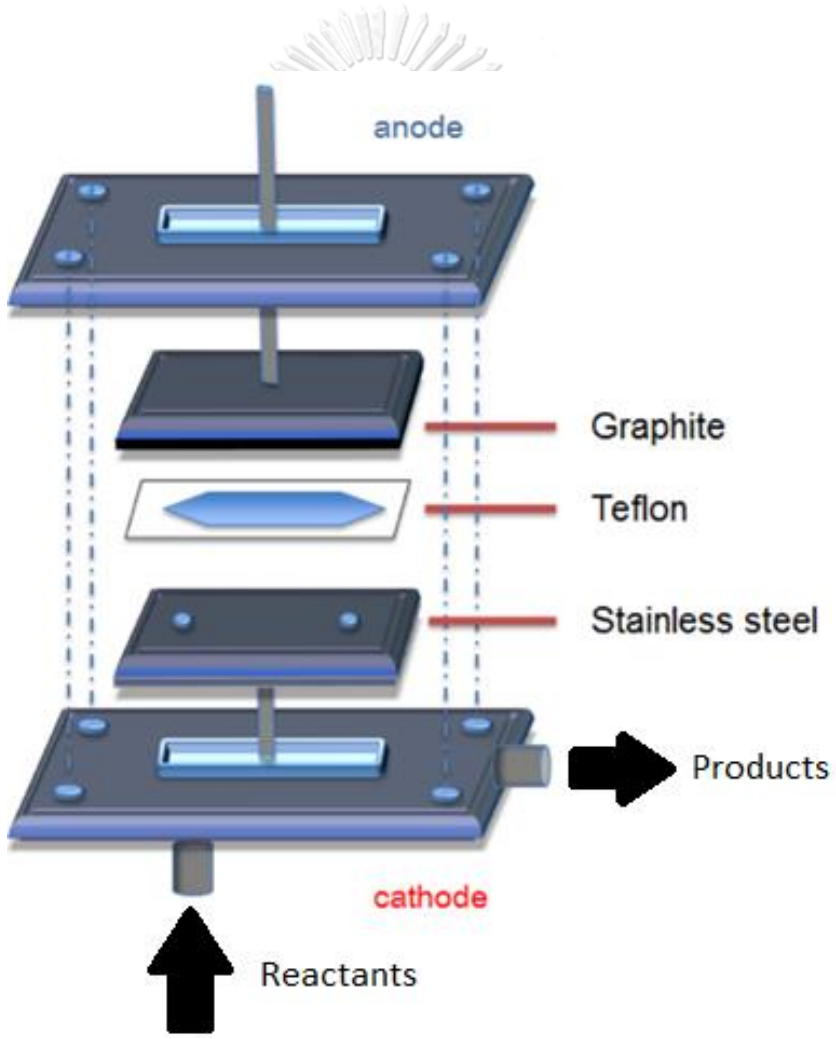


Figure 3.1 Schematic diagram of the microreactor

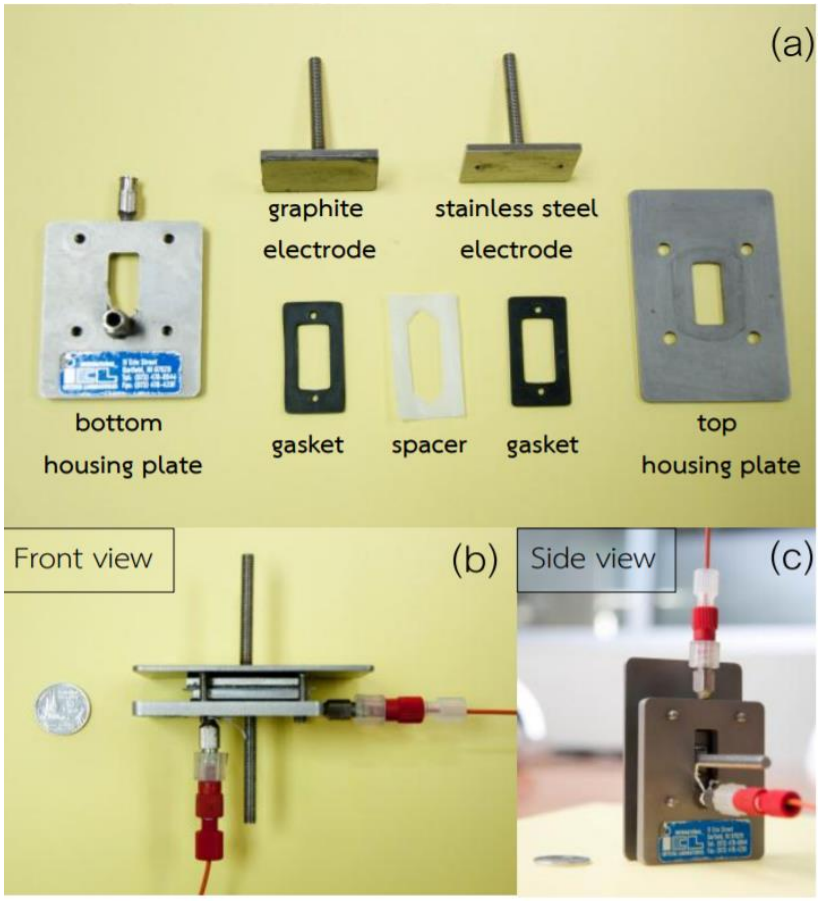


Figure 3.2 Images of (a) the components of the microreactor, (b) front view and (c) side view of the microreactor



### 3.1.4 Experiment setup

The schematic diagram and actual image of the experiment setup is as shown in Figure 3.3 and Figure 3.4 respectively. The apparatus or equipment needed for the experiment setup includes the DC power supply, syringe with syringe pump, microreactor, multimeter, connecting wires and product collection beaker. The syringe with the syringe pump will pump the reactants into the reactor through the bottom of the reactor after that, the products collected at the other end into the collection beaker. The DC power supply, microreactor and multimeter were linked together using the connecting wires to complete the circuit. The electrochemical

reaction was started by supplying direct current across the 2 electrodes. The first 0.5 mL of the solution leaving the reactor was discarded to ensure that the reactor was in steady state before collecting the products for sample analysis.

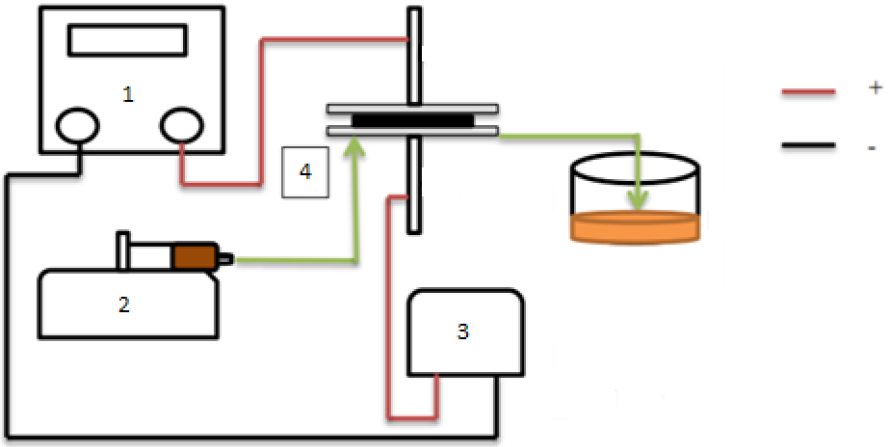


Figure 3.3 Schematic diagram of the experimental set up (1) Dc-power supply, (2) Syringe pump, (3) Multimeter, (4) Microreactor

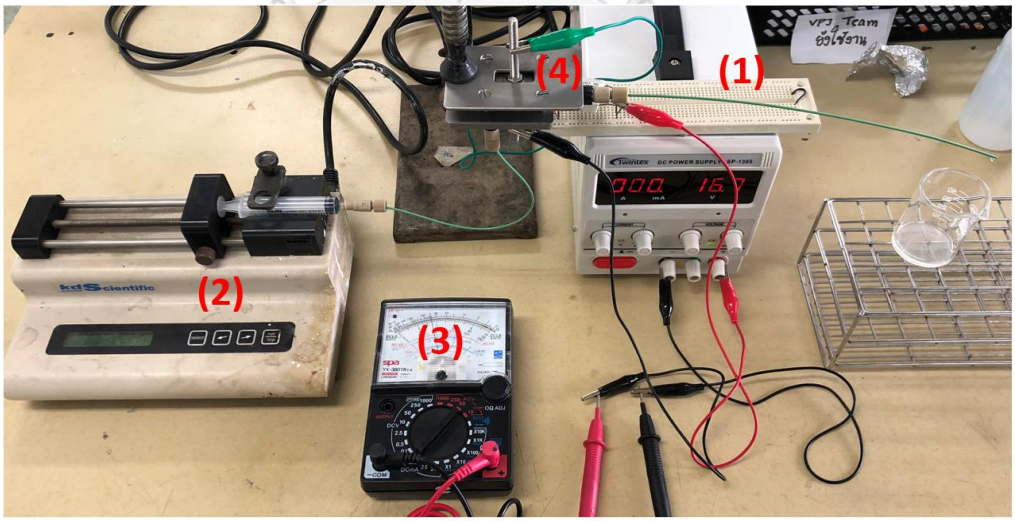


Figure 3.4 Image of the experimental set up (1) Dc-power supply, (2) Syringe pump, (3) Multimeter, (4) Microreactor

### 3.1.5 Lignin model compound

Benzyl phenyl ether (BPE) was used as the α-O-4 lignin model compound while a co-solvent system was used as the solvent. The concentration of BPE in the co-solvent entering the reactor at each experiment was fixed. The BPE was refrigerated during storage due to its low melting point of 39℃. The product collected from the reactor was kept away from sunlight and refrigerated as well during storage to prevent any alteration before analysis.

## 3.2 Research Methodology

This section presents the research methodology which were mainly branched into 2 including dissolution and degradation of the lignin model compound to achieve the objectives of the project.



### 3.2.1 Dissolution of lignin model compound

Before going towards the degradation or bond cleavage of the lignin model compound, the dissolution of the lignin model compound in the co-solvent system is needed to be investigated.

The parameter that was being varied to investigate the dissolution ability of the lignin model compound was:

1. Varying organic solvent volume fraction from 100 to 10 vol% in the co-solvent system.

### 3.2.2 Degradation of lignin model compound

After determining the dissolubility of the lignin model compound in the co-solvent system, the degradation performance of the lignin model compound in the co-solvent system was studied.

The parameters that were being varied to investigate the degradation performance of the lignin model compound in the co-solvent system using a microreactor were:

1. Residence time ranging from 27.0 to 81.0 seconds.
2. Current density ranging from 0.93 to 8.33 $A/m^2$.
3. Varying organic solvent volume fraction from 30 to 50 vol% in the co-solvent system.
4. Varying type co-solvent systems using ethanol/water and acetonitrile co-solvent systems.



## 3.3 Analytical instruments

This section presents the analytical instruments used for this research work to determine the dissolubility of the lignin model compound and the degradation performance of the lignin model compound. The details of each analytical instruments are as follows:

### 3.3.1 UV-Visible spectrophotometer

A UV-visible spectrophotometer (UV-Vis, UV-2600, Shimadzu, Kyoto, Japan) shown in Figure 3.5 was used to analyze the dissolution of BPE in co-solvent system and hydrogen peroxide ($H_2O_2$) concentration via UV absorption method at the Excellence in Particle and Technology Engineering laboratory in Chulalongkorn University, Thailand.

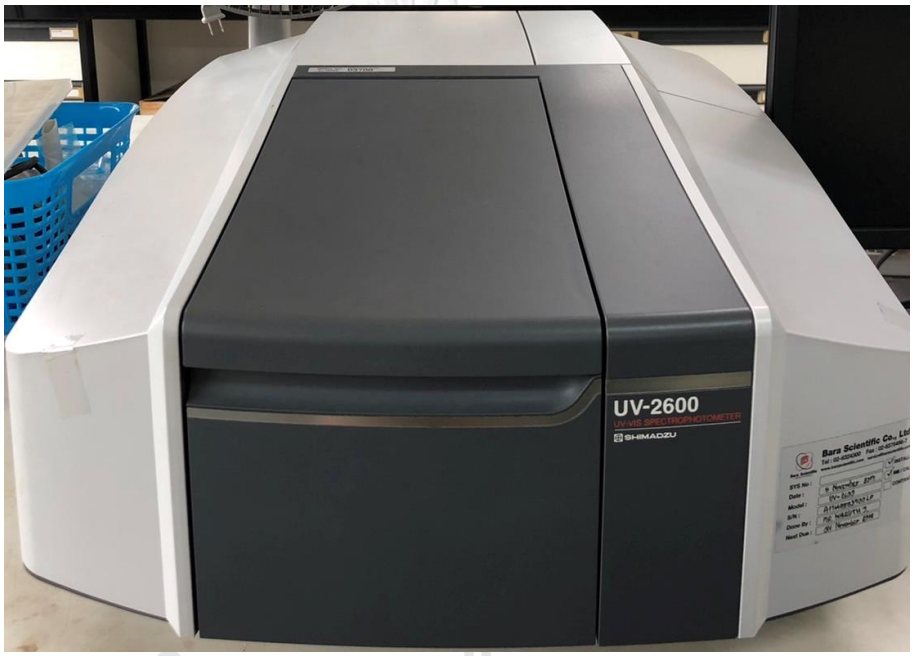




Figure 3.5 UV-Visible spectrophotometer

#### 3.3.1.1 Dissolution of BPE in co-solvent system analysis

The dissolution of BPE in a co-solvent system was analyzed using a UV-visible spectrophotometer. The wavelength scan ranges from 190nm to 900nm using a quartz cuvette to find a clear peak of BPE for each co-solvent system. The wavelength of 258nm was used for ethanol/water co-solvent system while wavelength of 242nm acetonitrile/water co-solvent system. The wavelengths were picked based on the most

linear graph gained for the standard graph of volume fraction of both organic solvent against absorption. The concentration of ethanol or acetonitrile in water was lowered until a sudden increase in absorption due clouding of the sample when BPE precipitates.

### 3.3.1.2 Concentration of hydrogen peroxide ($H_2O_2$) analysis

The concentration of hydrogen peroxide ($H_2O_2$) present in the samples were analyzed by mixing the 1 ml of the sample with 1 ml of solution A and solution B. The wavelength of 350nm was used to measure the concentration of $H_2O_2$ in the samples with deionized water used as the blank sample [29]. The steps of preparing solution A and solution B are as follows:

Table 3.1 Preparation of Solution A and Solution B [29]

| | |
|---|---|
| Solution A | 1. 0.01 g of ammonium molybdate, 0.1g of sodium hydroxide and 3.3 g of potassium iodide were weighed then added into a 50 ml volumetric flask.<br>2. Deionized water was added till 50 ml then mixed till complete dissolve. |
| Solution B | 1. 0.01 g of ammonium molybdate, 0.1g of sodium hydroxide and 3.3 g of potassium iodide were weighed then added into a 50 ml volumetric flask.<br>2. Deionized water was added till 50 ml then mixed till complete dissolve. |

### 3.3.2 Gas Chromatography

### 3.3.3 Gas Chromatography Mass Spectrometry (GC-MS)

The samples collected from the reactor were sent to the Scientific and Technological Research Equipment Center (STREC, Chulalongkorn University, Bangkok, Thailand) for product identification using a gas chromatography shown in Figure 3.6. The gas chromatography is coupled with a mass spectrometry (GC-MS, 7890 GC system, Agilent, Santa Clara, CA, USA) equipped with a HP-5ms column (Agilent, Santa Clara, CA, USA) 30 m × 0.25 mm × 0.25 μm. The samples after filtration were injected directly into the column without further dilution or purification. The temperature of the column oven was programmed from 100 ℃ holding for 3.0 minutes to 300 ℃ holding for 5.0 minutes at 6 ℃ $min^{-1}$. Helium was used as the carrier gas was set at a constant flow rate of 1.0 ml $min^{-1}$. The temperature of the injector and detector were set to 300 ℃ whereas the volume of injection was set to 2 μL in splitless mode. The compounds separated in the column were analyzed using the mass spectrometry. The products were sent through an ion source where the fragments were separated by a single quadrupole in the range of 33 to 500 m/z. The mass spectra collected were analyzed by comparing it with the spectra of pure compounds from commercial NIST2011 library.

Figure 3.6 Gas Chromatography Mass Spectrometry (GC-MS)

### 3.3.4 Gas Chromatography with Flame Ionization Detector (GC-FID)

The concentration of benzyl phenyl ether as the lignin model compound was analyzed at the Excellence in Particle and Technology Engineering laboratory in Chulalongkorn University, Thailand. The gas chromatography is coupled with a flame ionization detector (GC-FID, GC-14B, Shimadzu, Kyoto, Japan) equipped with a ZB-5 column (Phenomenex, Torrance, CA, USA) 60 m × 0.25 mm × 0.25 μm. The samples after filtration were injected directly into the column without further dilution or purification. The temperature of the column oven was programmed from 50 ℃ holding for 5.5 minutes to 290 ℃ holding for 7.5 minutes at 20 ℃ $min^{-1}$. Helium was used as the carrier gas. The temperature of the injector and detector were set to 290 ℃ whereas the volume of injection was set to 2 μL in splitless mode. The compounds separated in the column were detected using the flame ionization detector. The percentage of remaining benzyl phenyl ether as the lignin model compound in the sample after degradation was calculated using the equation (3.1).

$$Remaining\ BPE\ (\%) = \frac{Area\ of\ BPE\ after\ degradation}{Area\ of\ BPE\ before\ degradation} \times 100\% \quad (3.1)$$

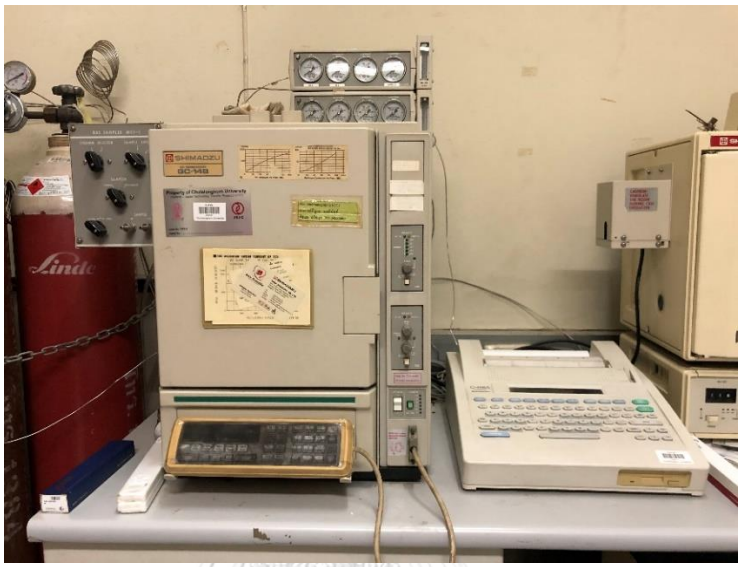


Figure 3.7 Gas Chromatography with Flame Ionization Detector (GC-FID)

### 3.3.5 Nuclear Magnetic Resonance Spectrometer (NMR)



The samples collected from the reactor were also sent to the Scientific and Technological Research Equipment Center (STREC, Chulalongkorn University, Bangkok, Thailand) for the confirmation of the presence of aliphatic compounds using a nuclear magnetic resonance spectrometer (NMR, Avance III HD/OXFORD 500 MHz, Bruker, Billerica, MA, USA) shown in Figure 3.8. The samples are diluted before analysis, diluting 500 µL of the sample with 100 µL of deuterium oxide ($D_2O$) for a total of 600 µL.


Figure 3.8 Nuclear Magnetic Resonance Spectrometer 500 MHz. (Liquid) – NMR 500 MHz.

# CHAPTER 4

# RESULTS AND DISCUSSION

The study of the degradation of benzyl phenyl ether (BPE) as the lignin model compound, was carried out using a microreactor via electrochemical advanced oxidation process (EAOP). This chapter consist of the following main parts:

1. Dissolution of benzyl phenyl ether as the lignin model compound.
2. Hydrogen peroxide production and degradation of benzyl phenyl ether via electrochemical advanced oxidation process in a microreactor
3. Identification of possible intermediate products and possible reaction pathway mechanism of BPE degradation by EAOP in a microreactor

## 4.1 Dissolution of benzyl phenyl ether as the lignin model compound



The dissolution of benzyl phenyl ether (BPE) as the lignin model compound was investigated in both ethanol/water ($EtOH/H_2O$) and acetonitrile/water ($MeCN/H_2O$) co-solvent systems. The investigation was carried by changing the volume fraction of ethanol or acetonitrile from 100% down to 10% in the co-solvent systems with concentration of BPE fixed at 100 mg/L. An UV-Vis spectrophotometer was used to determine the dissolubility of BPE in the co-solvent systems. BPE was deemed insoluble in the solution when a sharp increase in absorption is detected by the UV-Vis which indicates the precipitation of BPE. A co-solvent system was used because water is needed to generate hydroxyl radicals to degrade the α-O-4 bond between two aromatic rings in BPE via electrochemical advanced oxidation process (EAOP), while ethanol or acetonitrile is used to dissolve BPE as it is insoluble in pure

water. BPE need to be completely dissolved to not clog the reactor as solid particles can clog the tubes or even the microreactor itself.

### 4.1.1 Ethanol/water co-solvent system

The dissolution of BPE in the ethanol/water (EtOH/$H_2O$) co-solvent system was investigated by changing the volume fraction of ethanol to 10, 20, 30, 50 and 100% in the co-solvent system with concentration of BPE fixed at 100 mg/L. Based on Figure 4.1, the UV-vis absorption remains relatively constant when the volume fraction of EtOH in the EtOH/$H_2O$ co-solvent system decreases from 100% to 20%. However, when the volume fraction of ethanol drops to 10%, the adsorption sharply increases, indicating incomplete dissolution of BPE in the solvent. The mixture observed turns cloudy when the volume fraction of EtOH drops to 10% in the solution indicating that BPE has precipitated in the solution due to low EtOH concentration. Since the absorbance from 100% to 20% EtOH volume fraction is relatively constant, the absorbance change is being dominated by the clouding of the mixture rather than the change of BPE in the solution. The clouding of the mixture increases the opacity of the solution which reduces the light that can pass through; thus, increasing the absorption. Therefore, the data suggest that the minimum concentration of EtOH in the EtOH/H2O co-solvent system to dissolve 100 mg/L of BPE is 20 vol%. However, based on the literature survey conducted, according to Matsagar et al., EtOH volume fraction of 30% offers a good balance between solubility and conversion even though higher volume fraction of ethanol offers better solubility but comes at the cost of conversion [12]. Therefore, based on the data obtained and data reported in literatures, 30 vol% EtOH in the EtOH/$H_2O$ co-solvent system was chosen for the rest of the research for both solubility and convertibility unless stated otherwise.

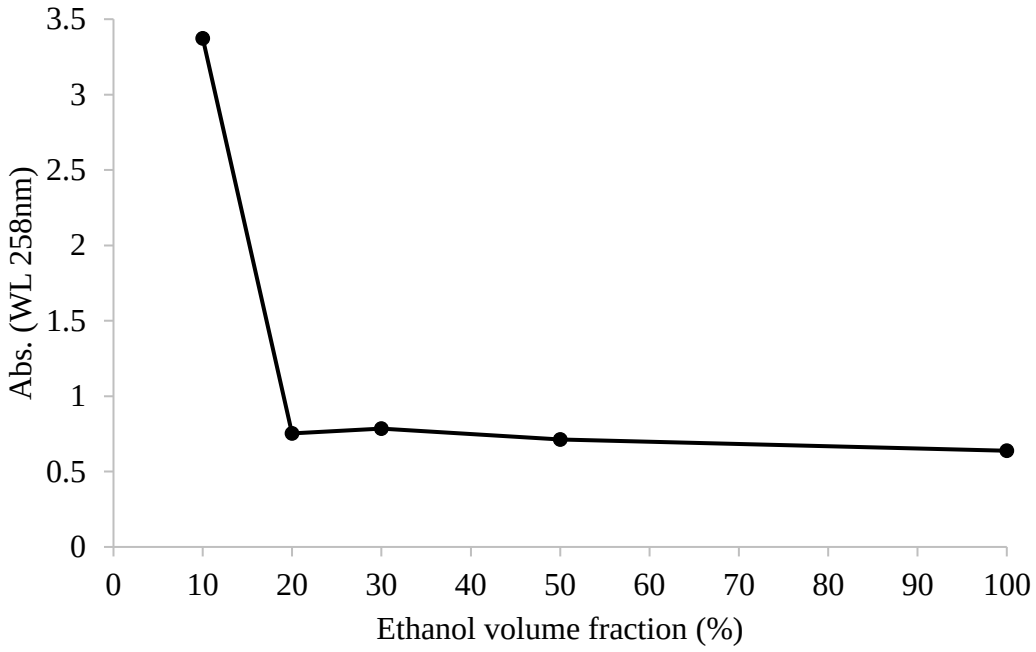


Figure 4.1 UV-vis absorption of different volume fraction of ethanol with concentration of BPE fixed at 100 mg/L

### 4.1.2 Acetonitrile/water co-solvent system



The dissolution of BPE in the acetonitrile/water (MeCN/H2O) co-solvent system was investigated by changing the volume fraction of acetonitrile to 10, 20, 30, mg/L. Based on Figure 4.2, the UV-vis absorption remains relatively constant when the volume fraction of MeCN in the MeCN/$H_2O$ co-solvent system decreases from 100% to 30%. However, when the volume fraction of acetonitrile drops to 20%, the adsorption increased slightly while a further decrease to 10% saw a sharp increase in the UV-vis absorption due to incomplete dissolution of BPE in the solvent. Similar case to the ethanol/water co -solvent system, the clouding of the mixture is observed when MeCN volume fraction drops to 20% indicating that BPE has precipitated in the solution due to low MeCN concentration. Since the absorbance from 100% to 30% MeCN volume fraction is also relatively constant, the absorbance change is being

dominated by the clouding of the mixture rather than the change of BPE in the solution. Like the ethanol/water co-solvent system, the clouding of the mixture increases the opacity of the solution which reduces the light that can pass through; thus, increasing the absorption. The data suggest that the minimum concentration of MeCN in the MeCN/$H_2O$ co-solvent system to dissolve 100 mg/L of BPE is 30 vol%. Therefore, based on the data obtained, 30 vol% MeCN in the MeCN/$H_2O$ co-solvent system was chosen for the rest of the research for both solubility and convertibility unless stated otherwise.

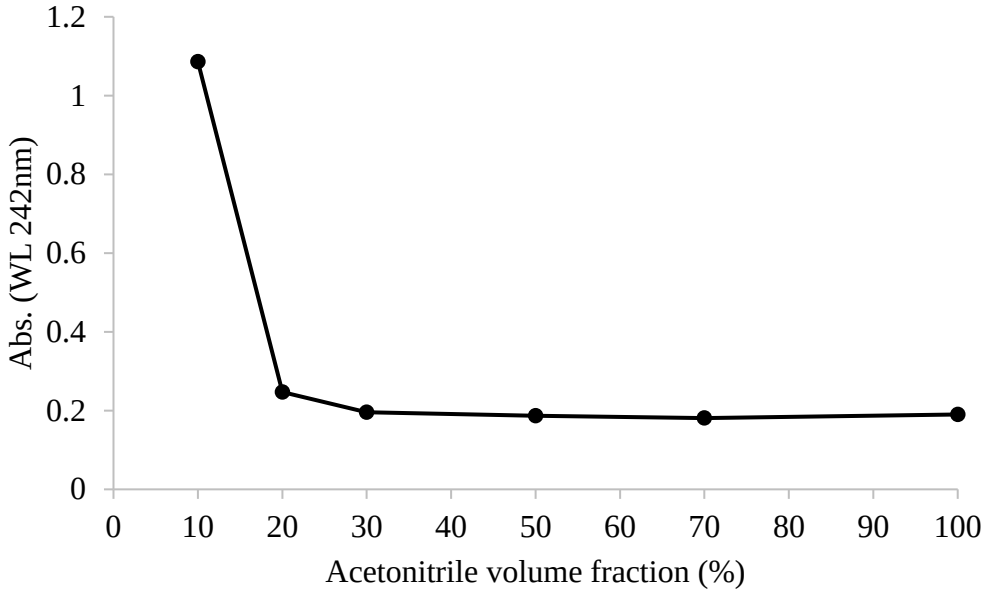


Figure 4.2 UV-vis absorption of different volume fraction of acetonitrile with concentration of BPE fixed at 100 mg/L

## 4.2 Hydrogen peroxide production and degradation of benzyl phenyl ether via electrochemical advanced oxidation process in a microreactor

Characteristics of electrochemical advanced oxidation process in a microreactor for benzyl phenyl ether degradation and hydrogen peroxide production are discussed. The effect of mean residence time, applied current, concentration of solvent and type of solvent are the main varying parameters discussed.

### 4.2.1 Characteristics of BPE degradation and effect of residence time by EAOP in a microreactor

The degradation of BPE starts when the current from the power supply is switched on forming hydroxyl radicals (OH*) from the oxidation or dissociation of water through Eq. (4.1). The fixed concentration of BPE entering the inlet of the reactor will be degraded by the hydroxyl radicals formed in the reactor resulting in the lower concentration of BPE at the outlet of the reactor. However, due to the OH* being reactive, it is rarely found in the reaction media as it reacts with other components through Eq. (4.2) and Eq. (4.3). The compounds that OH* can react with is the BPE compound as well through Eq. (4.4) resulting in mineralization of BPE. Therefore, hydrogen peroxide ($H_2O_2$) can be found as one of products in the product stream. The concentration of $H_2O_2$ in the product stream can be measured using a UV-vis spectrometry via the colorimetric method.



$$H_2O \rightarrow OH^* + H^+ + e^- \quad (4.1)$$

$$OH^* + OH^* \rightarrow H_2O_2 \quad (4.2)$$

$$H_2O_2 + OH^* \rightarrow H_2O + HO_2^* + H_2O \quad (4.3)$$

$$\text{Compound} + OH^* \rightarrow \text{Compound minerization products} \quad (4.4)$$

Figure 4.3 shows the concentration of hydrogen peroxide ($H_2O_2$) with varying flowrate at 3, 5, 7 and 9 ml/h giving a mean residence time of 81.0, 48.6, 34.7 and 27.0 seconds with current at 1.25mA or current density of 4.63 A/m$^2$. Based on Figure

4.3, when only ethanol/water co-solvent system is supplied to the microreactor, the concentration of $H_2O_2$ measured was 0.104 mg/L whereas for the ethanol/water co-solvent system with 100 mg/L of BPE, the concentration of $H_2O_2$ measured was 0.050 mg/L. The result showing the decrease in $H_2O_2$ concentration is the result of the hydroxyl radicals degrading the BPE present in the solution. The degradation of BPE and the formation of $H_2O_2$ are competing with each other for hydroxyl radicals as shown in Eq. (4.2) and Eq. (4.4).

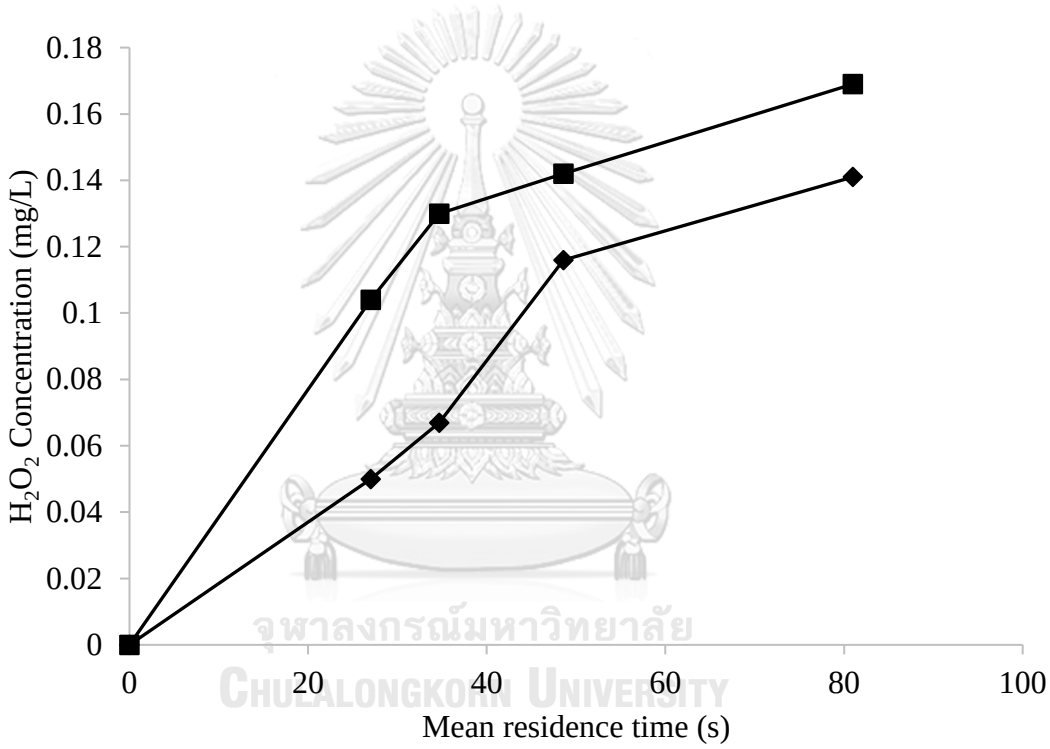




Figure 4.3 Concentration of hydrogen peroxide in the product stream via EAOP under fixed current applied of 1.25 mA at mean residence time of 27.0, 34.7, 48.6 and 81.0 seconds; (■) in ethanol/water co-solvent system and (♦) in 100ppm BPE ethanol/water co-solvent system

Furthermore, the results in Figure 4.3 shows that as the mean residence time increase for both with and without BPE in the ethanol/water co-solvent systems, the concentration of $H_2O_2$ increases which also equates to the increase in hydroxyl

radicals in the reactor as well. Therefore, based on Figure 4.4, the degradation of fixed BPE concentration of 100 mg/L in the ethanol/water co-solvent system with current at 1.25mA or current density of 4.63 A/m$^2$, the degradation increased from 57.07% to 90.60% when the mean residence time increased from 27.0 seconds to 81.0 seconds. This is mainly due to more hydroxyl radicals being generated and BPE in the solution being exposed to the hydroxyl radicals for a longer period of time as the mean residence time increases.

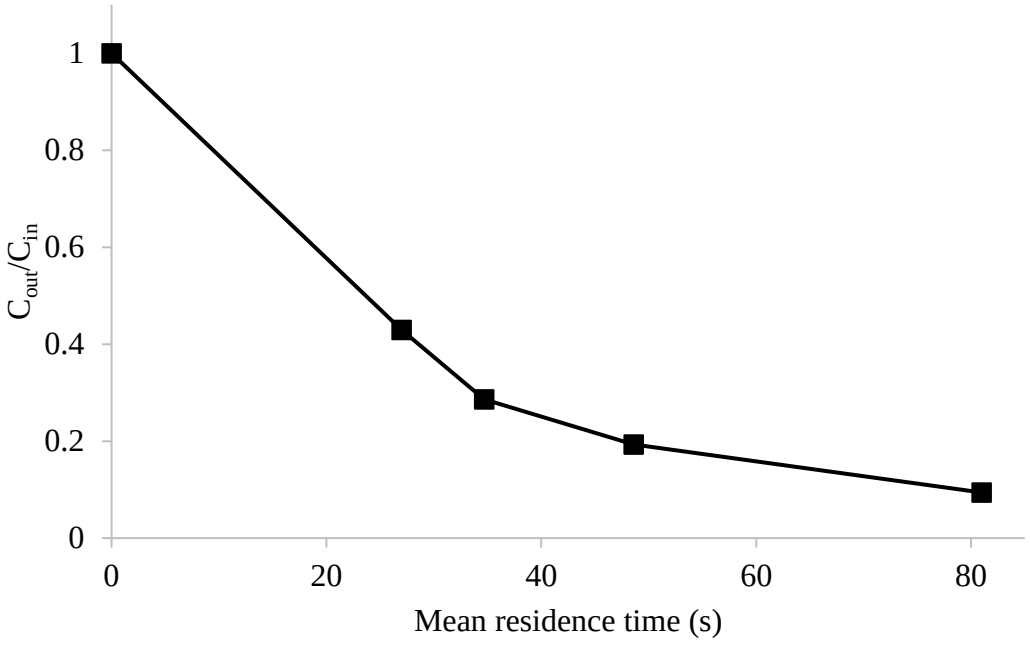


Figure 4.4 Degradation of 100 mg/L BPE in ethanol/water co-solvent system via EAOP at applied current of 1.25 mA at mean residence times of 27.0, 34.7, 48.6 and 81.0 seconds

The data obtained in Figure 4.4 were then fitted to the pseudo first order model to determine the reaction rate of BPE degradation; the data were fitted in the form of Eq. (4.5). $C_{in}$, $C_{out}$, $t$ and $k$ are the inlet concentration of BPE, outlet concentration of BPE, mean residence time (s), and rate constant ($s^{-1}$) respectively. The data obtained were fitted to the pseudo first order model with $R^2 > 0.99$ as shown

in Figure 4.5. The degradation of BPE was found to be well represented by the pseudo first order kinetics with $3.11 \times 10^{-2}$ $s^{-1}$ being the reaction rate constant.

$$\ln\left(\frac{C_{in}}{C_{out}}\right) = kt \tag{4.5}$$

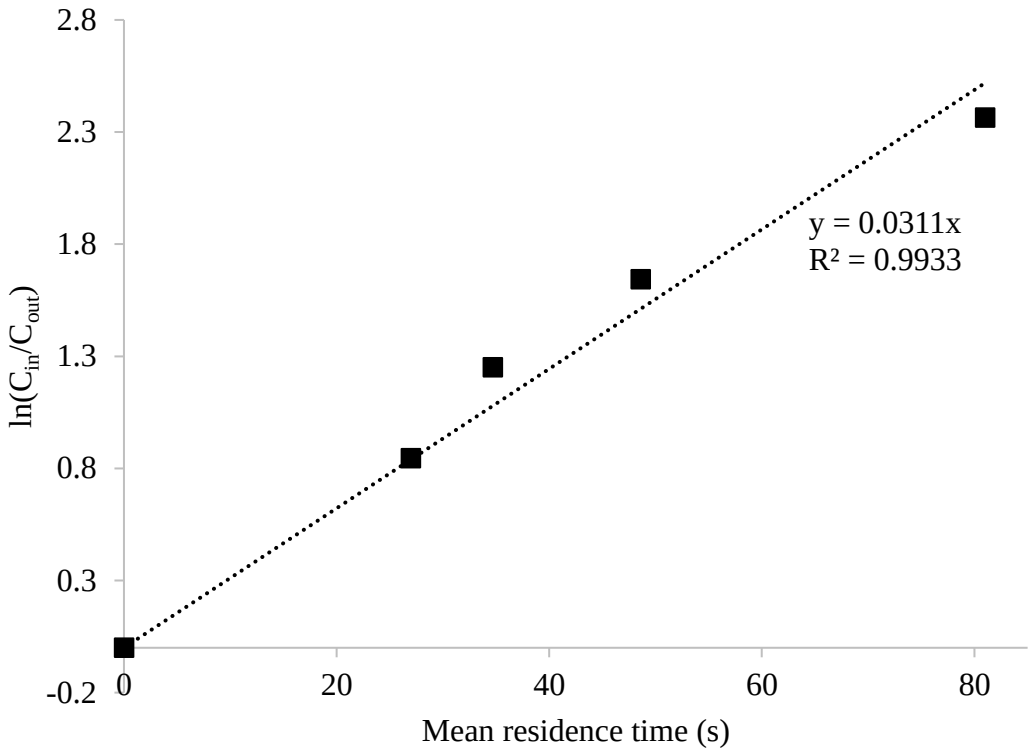


Figure 4.5 Kinetic plot of BPE degradation in ethanol/water co -solvent system via EAOP at mean residence times of 27.0, 34.7, 48.6 and 81.0 seconds at applied current of 1.25 mA

Another graph was plotted using the reaction rate constant (k) obtained from Figure 4.5 and using Eq. (4.5) to obtain Figure 4.6 which compares the model and the experimental data. The degradation of BPE experimental data was found to be well represented by the simple kinetic model with $R^2$ = 0.9931 which indicates that the kinetics in the reactor of the system dominates transport phenomena.

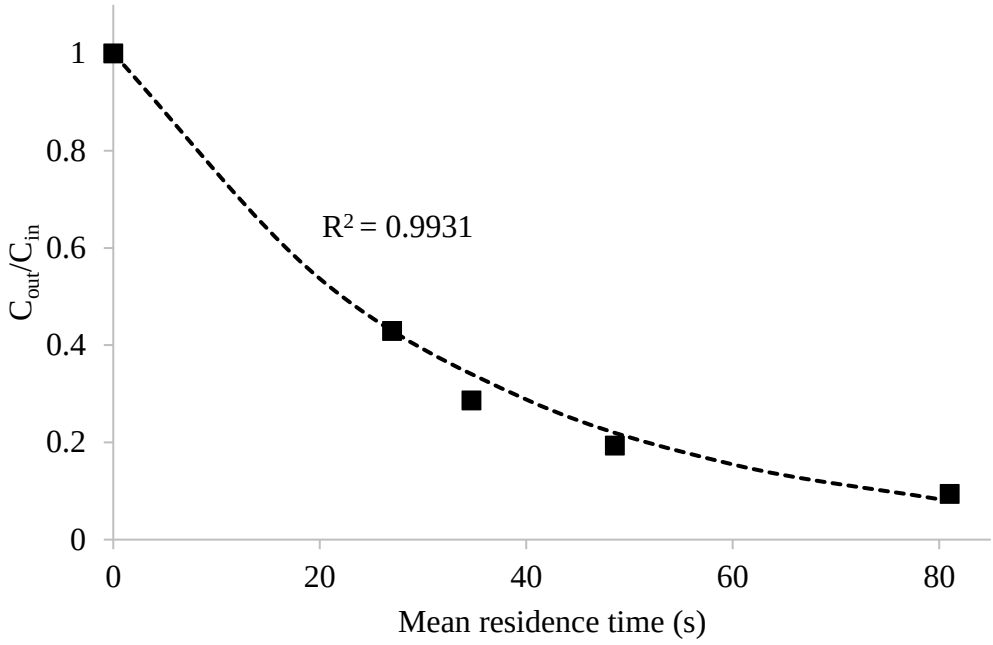


Figure 4.6 The model (---) plotted with the experimental data (■)



### 4.2.2 Effect of applied current on BPE degradation by EAOP in a microreactor

The current or current density applied to the microreactor when undergoing EAOP is one of the parameters affecting the degradation of BPE in the co-solvent system. Figure 4.7 shows the degradation of BPE in 30 vol% ethanol ethanol/water co-solvent system with varying flowrate at 3, 5, 7 and 9 ml/h giving a mean residence time of 81.0, 48.6, 34.7 and 27.0 seconds with current at 0.25, 1.25 and 2.25 mA giving current density of 0.93, 4.63 and 8.33 $A/m^2$. When comparing the degradation of BPE under a constant mean residence time for example at 81.0 seconds, the percentage of BPE degraded are 65.68%, 90.60% and 96.97% when the current applied are at 0.25, 1.25 and 2.25 mA respectively. The concentration of hydrogen peroxide without BPE present for applied current of 1.25 and 2.25 mA shows a similar trend in Figure 4.8 where the hydrogen peroxide concentration for 2.25 mA

produced is higher at 0.198 mg/L whereas 1.25mA at 0.169 mg/L in mean residence time of 81.0 seconds; thus, giving a higher degradation percentage.

Even though the applied current is almost doubled from 1.25 mA to 2.25 mA, the degradation of BPE and the production of hydrogen peroxide does not increase significantly when compared with each other. From observation when conducting the experiment, there were more gas bubbles being produced when 2.25 mA current is applied when compared to 1.25 mA. These bubbles produced are suspected to be oxygen produced through oxygen evolution shown in Eq. (4.6) or hydrogen peroxide direct discharge shown in Eq. (4.7) or reaction of hydrogen peroxide with hydroxyl radicals shown in Eq. (4.8) [31], [32]. The gas bubbles produced in the reactor will create film regions that completely shuts down the electrochemical transformation in those regions which lowers the efficiency of the reactor [33]. Therefore, the difference between applied current of 1.25 and 2.25 mA even though almost doubled is not as significant.

Furthermore, focusing on the degradation of BPE on applied current of 0.25 mA or current density of 0.93 $A/m^2$, the degradation can be observed with percentages of 41.01%, 50.36%, 58.37% and 65.68% at mean residence time of 27.0, 34.7, 48.6 and 81.0 seconds respectively. Even though the current applied is significantly lower compared to the other currents applied, a high degradation percentage can still be observed due to the low bond strength of the α-O-4 bond present in benzyl phenyl ether. Based on Figure 4.9, the α-O-4 bond have the lowest average bond-dissociation energies (BDEs) compared to other common bonds found in lignin such as β-O-4, β−1 and β-5 bonds which makes the α-O-4 bond the easiest to break as it requires the lowest energy to break it.

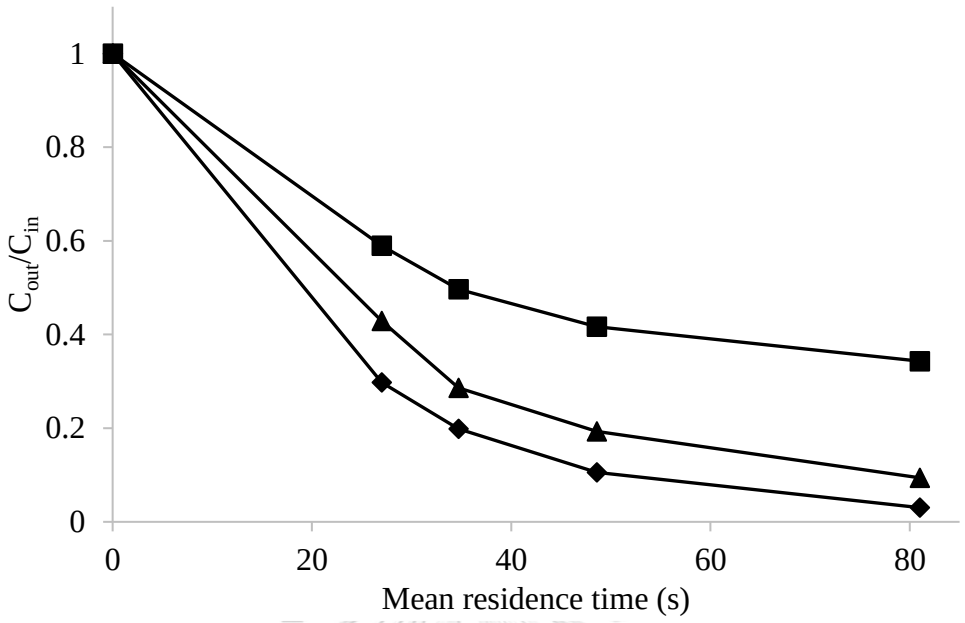


Figure 4.7 Degradation of BPE in ethanol/water co -solvent system via EAOP at mean residence time of 27.0, 34.7, 48.6 and 81.0 seconds at varying current applied; (■) I = 0.25mA, (▲) I= 1.25mA and (♦) I = 2.25mA

$$2H_2O \rightarrow O_2 + 4H^+ + 4e^- \quad (4.6)$$

$$H_2O_2 \rightarrow O_2 + 2H^+ + 2e^- \quad (4.7)$$

$$H_2O_2 + 2OH^* \rightarrow O_2 + 2H_2O \quad (4.8)$$

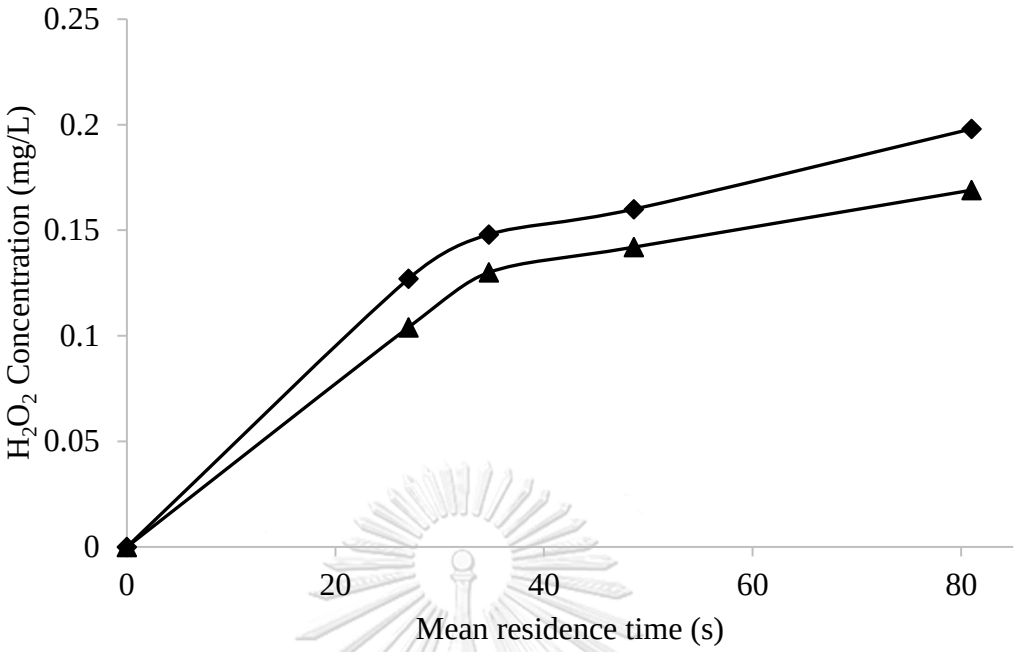


Figure 4.8 Concentration of hydrogen peroxide production in ethanol/water co - solvent system without BPE at mean residence time of 27.0, 34.7, 48.6 and 81.0 seconds at varying current applied; (▲) I= 1.25mA and (♦) I = 2.25mA

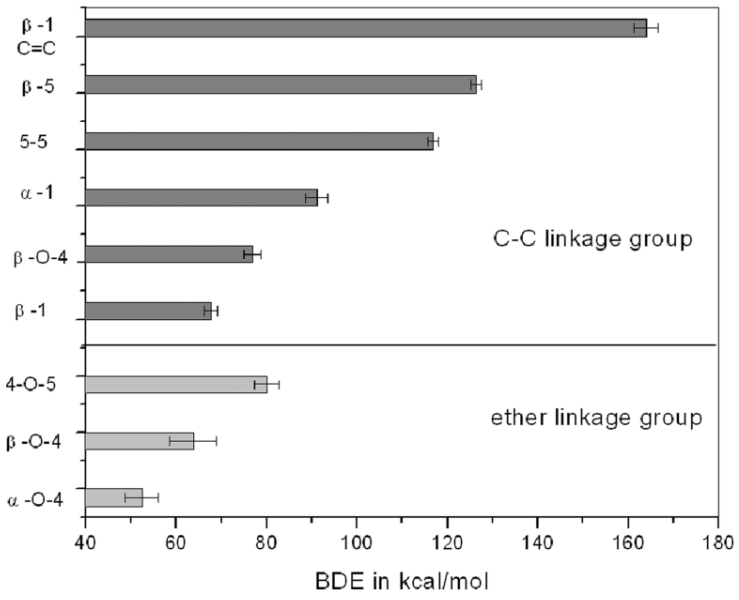


Figure 4.9 Comparison of average bond-dissociation energies (BDEs) for common lignin bonds. [34]

Furthermore, the data obtained from Figure 4.7 were also fitted to the pseudo first order model to determine the reaction rate of BPE degradation; the data were fitted in the form of Eq. (4.5). The data obtained were fitted to the pseudo first order model with $R^2 > 0.95$ across all mean residence time indicating a good fit as shown in Figure 4.10. The degradation of BPE was found to be well represented by the pseudo first order kinetics with $1.55 \times 10^{-2}$, $3.11 \times 10^{-2}$ and $4.43 \times 10^{-2}$ $s^{-1}$ being the reaction rate constant for applied currents of 0.25, 1.25 and 2.25 mA respectively. As all the data from Figure 4.7 have good fittings in the pseudo first order model, it can be concluded that the change in applied current to the reactor does not affect the order of the reaction.

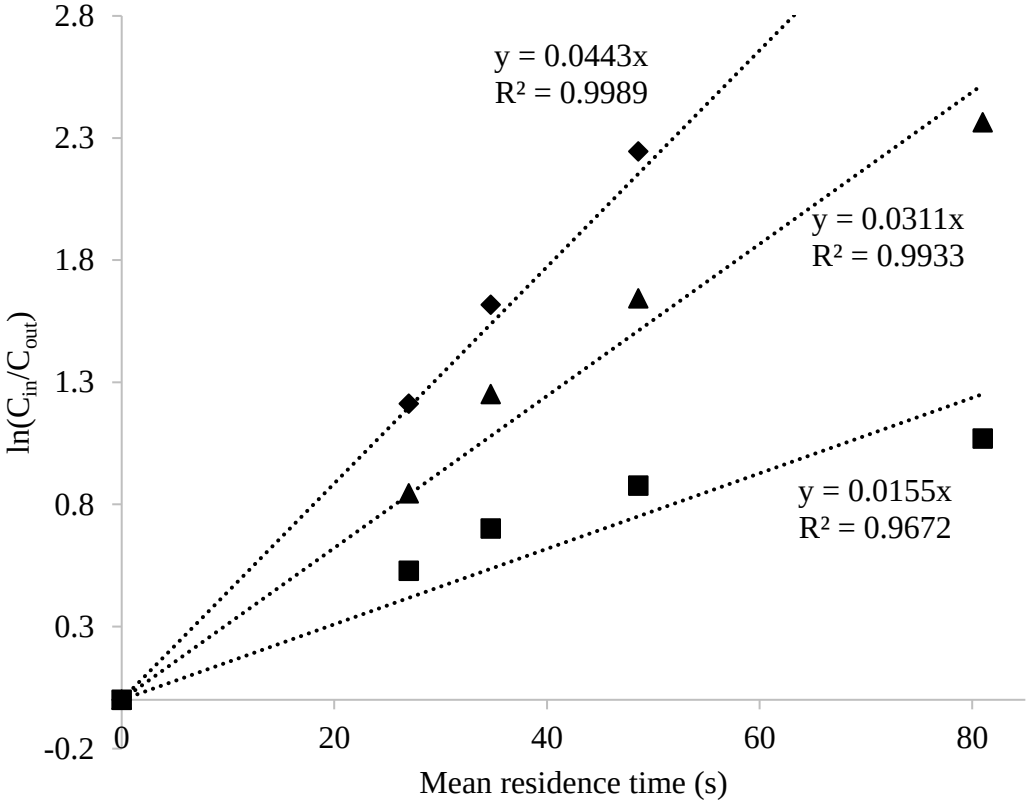


Figure 4.10 Kinetic plot of BPE degradation in ethanol/water co -solvent system via EAOP at mean residence times of 27.0, 34.7, 48.6 and 81.0 seconds at varying applied currents; (■) I = 0.25mA, (▲) I= 1.25mA and (♦) I = 2.25mA

### 4.2.3 Effect of solvent concentration on BPE degradation by EAOP in a microreactor

The concentration of the solvent used to dissolve BPE in the co-solvent system is also another parameter that can affect the degradation of BPE via EAOP in the microreactor. Figure 4.11 shows the degradation of BPE in ethanol/water co-solvent system at varying concentration of ethanol at 30 and 50 vol% at varying flowrate of 3, 5, 7 and 9 ml/h giving a mean residence time of 81.0, 48.6, 34.7 and 27.0 seconds with current fixed at 1.25 mA giving current density of 4.63 $A/m^2$. The degradation of BPE in 30 vol% ethanol is at 57.07%, 71.39%, 80.67% and 90.60% is higher than in 50 vol% ethanol at 47.66%, 54.31%, 64.06% and 79.34% % at mean residence time of 27.0, 34.7, 48.6 and 81.0 seconds respectively. The concentration of hydrogen peroxide without BPE present for 30 and 50 vol% ethanol showed similar trend in Figure 4.12 where the concentration of hydrogen peroxide for 30 vol% ethanol produced is higher than 50 vol% ethanol; thus, giving a higher degradation percentage. Ethanol is regarded as a very strong hydroxyl radicals scavenger [35], [36]. Therefore, the increase in the concentration of ethanol into the system will increase the competition for hydroxyl radicals between the ethanol and benzyl phenyl ether; thus lowering the degradation of BPE in the system.

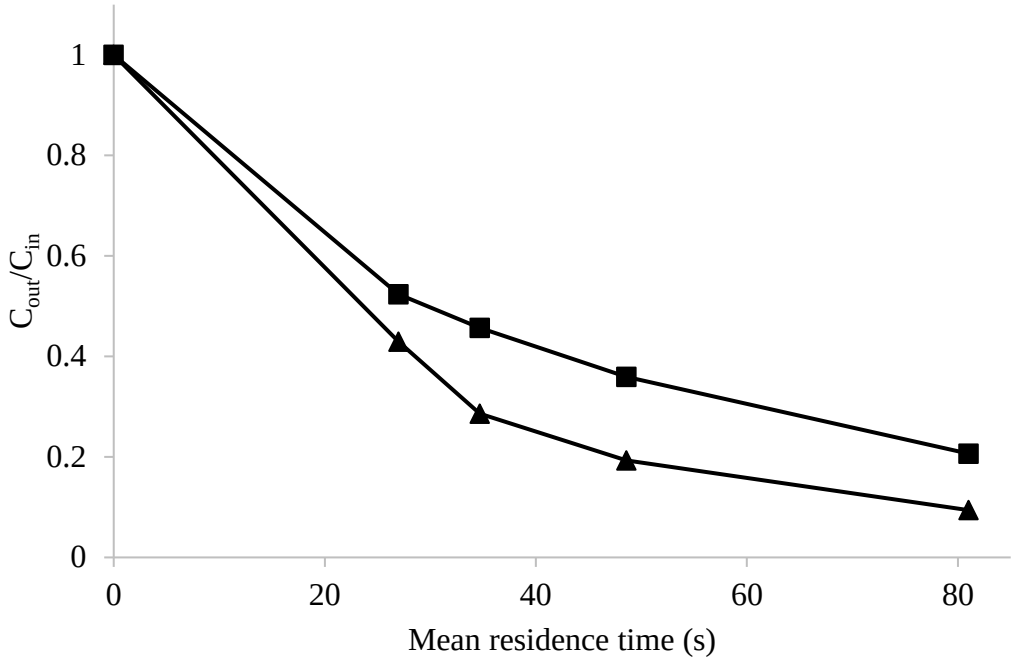


Figure 4.11 Degradation of BPE via EAOP at mean residence time of 27.0, 34.7, 48.6 and 81.0 seconds at fixed current applied of 1.25 mA at varying ethanol concentration in ethanol/water co-solvent system; (■) 50 vol% EtOH and (▲) 30 vol% EtOH



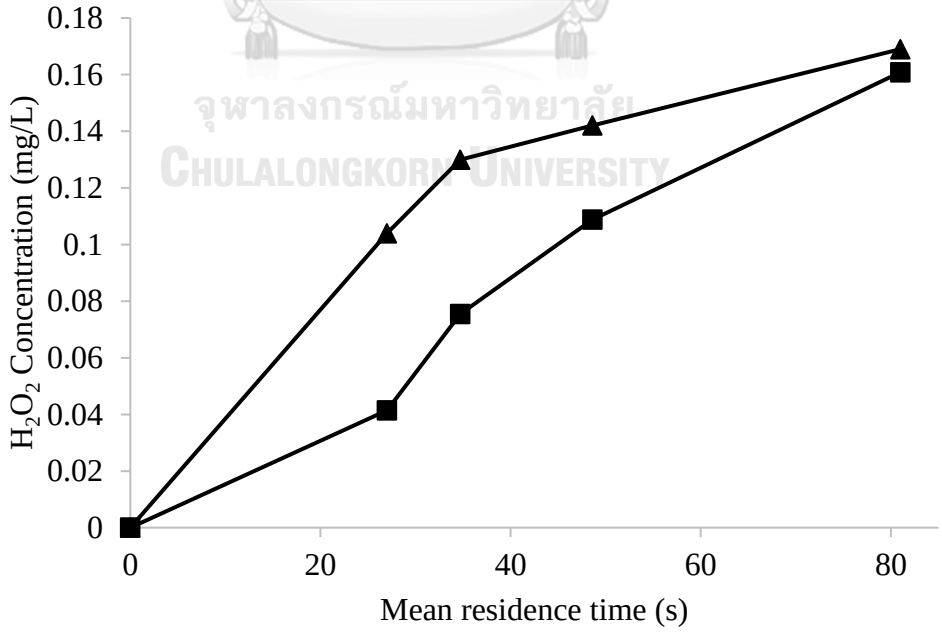


Figure 4.12 Concentration of hydrogen peroxide production without BPE at mean residence time of 27.0, 34.7, 48.6 and 81.0 seconds at fixed current applied of 1.25

mA at varying ethanol concentration in ethanol/water co-solvent system; (■) 50 vol% EtOH and (▲) 30 vol% EtOH

Furthermore, the data obtained from Figure 4.11 were also fitted to the pseudo first order model. The data obtained were fitted to the pseudo first order model with $R^2 > 0.99$ for both 30 and 50 vol% ethanol indicating a good fit as shown in Figure 4.13. The degradation of BPE was still found to be well represented by the pseudo first order kinetics with $3.11 \times 10^{-2}$ and $2.05 \times 10^{-2}$ $s^{-1}$ being the reaction rate constant for 30 and 50 vol% ethanol respectively. As all the data from Figure 4.13 have good fittings in the pseudo first order model, it can be concluded that the change in ethanol concentration in the co-solvent system does not affect the order of the reaction.

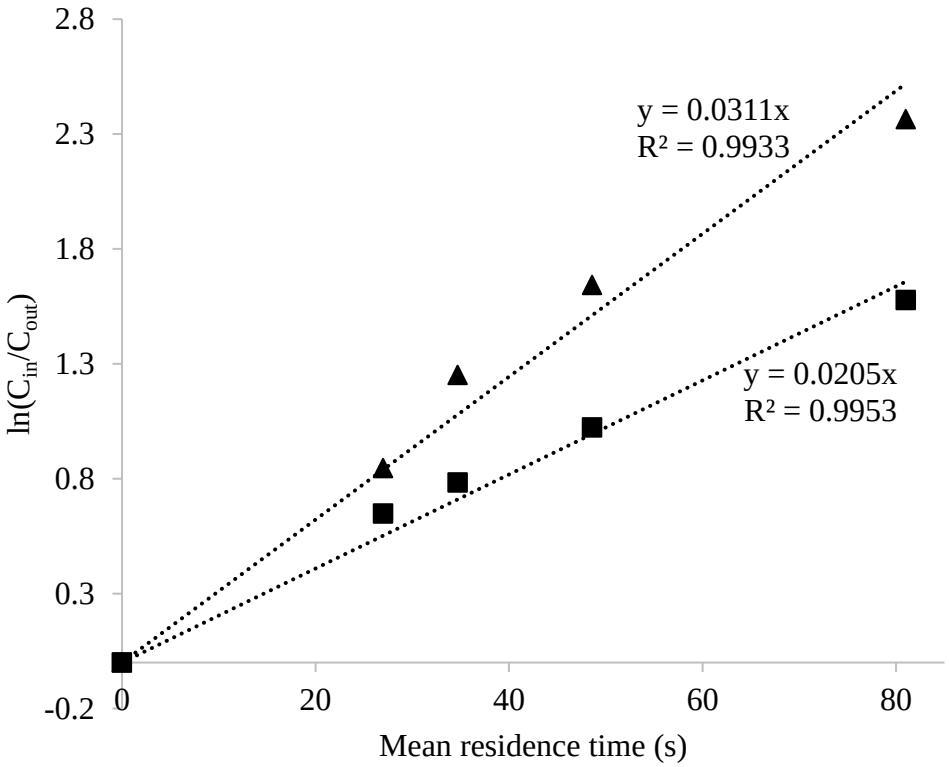


Figure 4.13 Kinetic plot of BPE degradation via EAOP at mean residence times of 27.0, 34.7, 48.6 and 81.0 seconds at fixed current applied of 1.25 mA at varying

ethanol concentration in ethanol/water co-solvent system; (■) 50 vol% EtOH and (▲) 30 vol% EtOH

### 4.2.4 Effect of type of solvent on BPE degradation by EAOP in a microreactor

As discussed briefly in the previous section, ethanol is a very strong hydroxyl radical scavenger, this section investigates the effect of different solvent in the co-solvent affecting the degradation of BPE via EAOP in the microreactor. Based on Figure 4.14, ethanol is the strongest hydroxyl radicals scavenger among the solvent listed so in order to investigate the effect of ethanol on degradation of BPE, acetonitrile is chosen for comparison as it shows similarity to ethanol in terms of solubility to BPE and water but acetonitrile is a less potent hydroxyl radicals scavenger [36]. Figure 4.15 shows the degradation of BPE in varying co-solvent system at acetonitrile and ethanol at varying flowrate of 3, 5, 7 and 9 ml/h giving a mean residence time of 81.0, 48.6, 34.7 and 27.0 seconds with current fixed at 1.25 mA giving current density of 4.63 $A/m^2$. The degradation of BPE in 30 vol% ethanol at 57.07%, 71.39%, 80.67% and 90.60% is lower than in 30 vol % acetonitrile at 64.34%, 74.17%, 85.53% and 95.00% % at mean residence time of 27.0, 34.7, 48.6 and 81.0 seconds respectively. The concentration of hydrogen peroxide without BPE present for acetonitrile and ethanol showed similar trend in Figure 4.15 where the concentration of hydrogen peroxide for acetonitrile produced is higher than ethanol; thus, giving a higher degradation percentage.

Another observation that can be observed is that even though the organic solvent used in the co-solvent system is switched from ethanol, a very strong hydroxyl radical scavenger to acetonitrile, a weaker hydroxyl radical scavenger, the degradation between both across all mean residence time is only 2.78 to 7.27% difference. The effectiveness of ethanol in being a hydroxyl radical scavenger is almost 10 times as potent as acetonitrile as the $IC_{50}$ for ethanol is 1.86 μL and acetonitrile is 17.5 μL. A hypothesis has been made to explain this observation is that there is a concentration

gradient of BPE across the cross-sectional area of the reactor once the potential is applied to the reactor. BPE assumed to be non-polar will be attracted to the non-polar hydrophobic graphite anode in the reactor. Since hydroxyl radicals are being generated at the graphite anode, BPE compounds even at much lower concentration than ethanol in the solution are able to compete with ethanol to react with the hydroxyl radicals being generated because most of the BPE compounds in the reactor are hypothesized to be near to the graphite anode. However, this hypothesis was not proven experimentally in this research.

| Solvent | $IC_{50}$ (μl in 800 μl) | Type | Solvent | $IC_{50}$ (μl in 800 μl) | Type |
|---|---|---|---|---|---|
| Ethanol | $1.86 \pm 0.13^{a}$ | Very strong | Chloroform | $26.0 \pm 2.44^{h}$ | Moderate |
| Methanol | $2.11 \pm 0.25^{a}$ | Very strong | Carbon tetrachloride | $47.0 \pm 3.56^{i}$ | Moderate |
| THF | $3.08 \pm 0.89^{b}$ | Very strong | Dichloromethane | $49.0 \pm 3.52^{j}$ | Moderate |
| DMF | $4.25 \pm 0.69^{b}$ | Very strong | Toluene | $57.7 \pm 3.54^{k}$ | Moderate |
| Diethyl ether | $4.17 \pm 1.06^{c}$ | Very strong | Benzene | $57.9 \pm 7.66^{k}$ | Moderate |
| Ethyl acetate | $5.44 \pm 1.28^{d}$ | Very strong | Cyclohexane | $66.9 \pm 5.99^{l}$ | Moderate |
| DMSO | $5.76 \pm 0.76^{d}$ | Very strong | Petroleum ether | $119 \pm 5.56^{m}$ | Weak |
| Acetone | $12.7 \pm 0.33^{e}$ | Strong | *n*-Hexane | $407 \pm 13.3^{n}$ | Weak |
| Carbon disulphide | $15.3 \pm 0.86^{f}$ | Strong | | | |
| Acetonitrile | $17.5 \pm 1.67^{g}$ | Strong | | | |

Figure 4.14 Hydroxyl radicals scavenger strength of organic solvents. $IC_{50}$ is the volume (μl) of 50% hydroxyl radical inhibition in the 800 μl reaction system. [36]

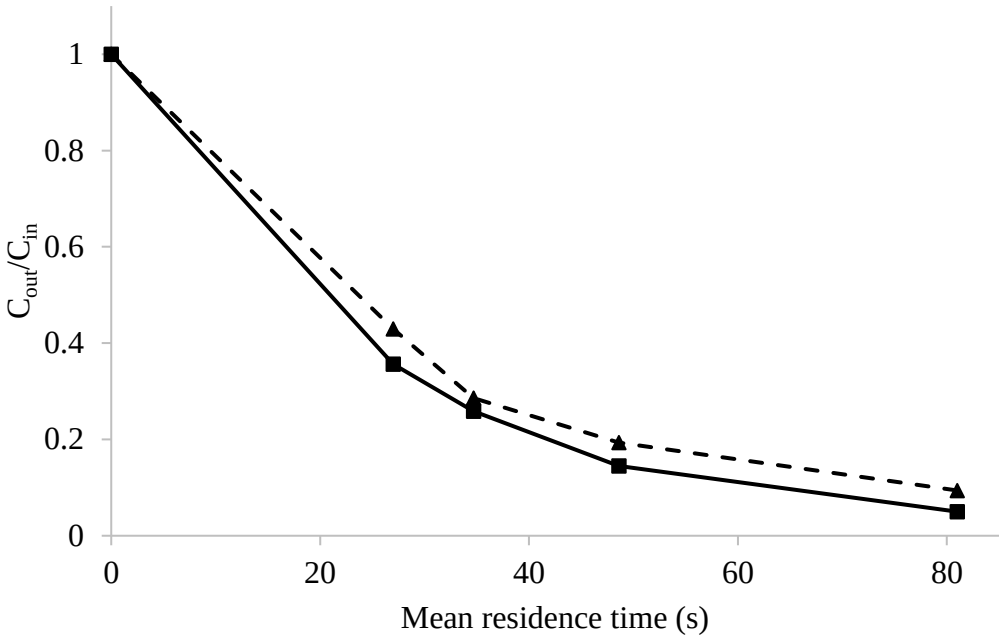


Figure 4.15 Degradation of BPE via EAOP at mean residence time of 27.0, 34.7, 48.6 and 81.0 seconds at fixed current applied of 1.25 mA at varying co-solvent systems; (■) MeCN/$H_2O$ and (▲) EtOH/$H_2O$



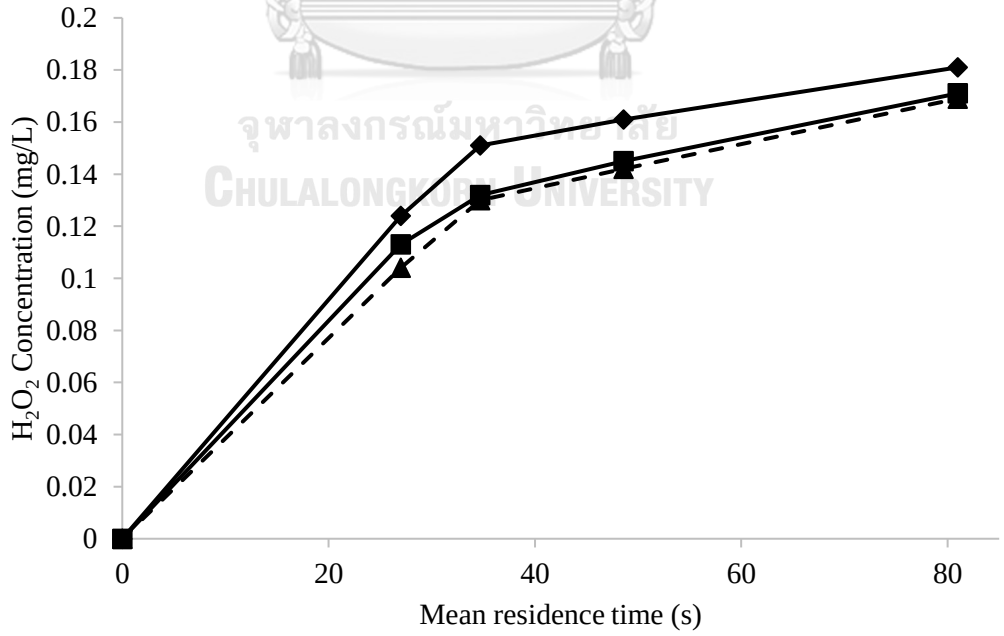


Figure 4.16 Concentration of hydrogen peroxide production without BPE at mean residence time of 27.0, 34.7, 48.6 and 81.0 seconds at fixed current applied of 1.25

mA at varying ethanol concentration in at varying solvent systems; (♦) $H_2O$, (■) $MeCN/H_2O$ and (▲) $EtOH/H_2O$

Furthermore, the data obtained from Figure 4.15 were also fitted to the pseudo first order model. The data obtained were fitted to the pseudo first order model with $R^2 > 0.99$ for both acetonitrile and ethanol co-solvent system indicating a good fit as shown in Figure 4.17. The degradation of BPE was still found to be well represented by the pseudo first order kinetics with $3.11 \times 10^{-2}$ and $3.79 \times 10^{-2}$ $s^{-1}$ being the reaction rate constant for ethanol and acetonitrile co-solvent system respectively. As all the data from Figure 4.17 have good fittings in the pseudo first order model, it can be concluded that the change in type of solvent in the co-solvent system does not affect the order of the reaction.

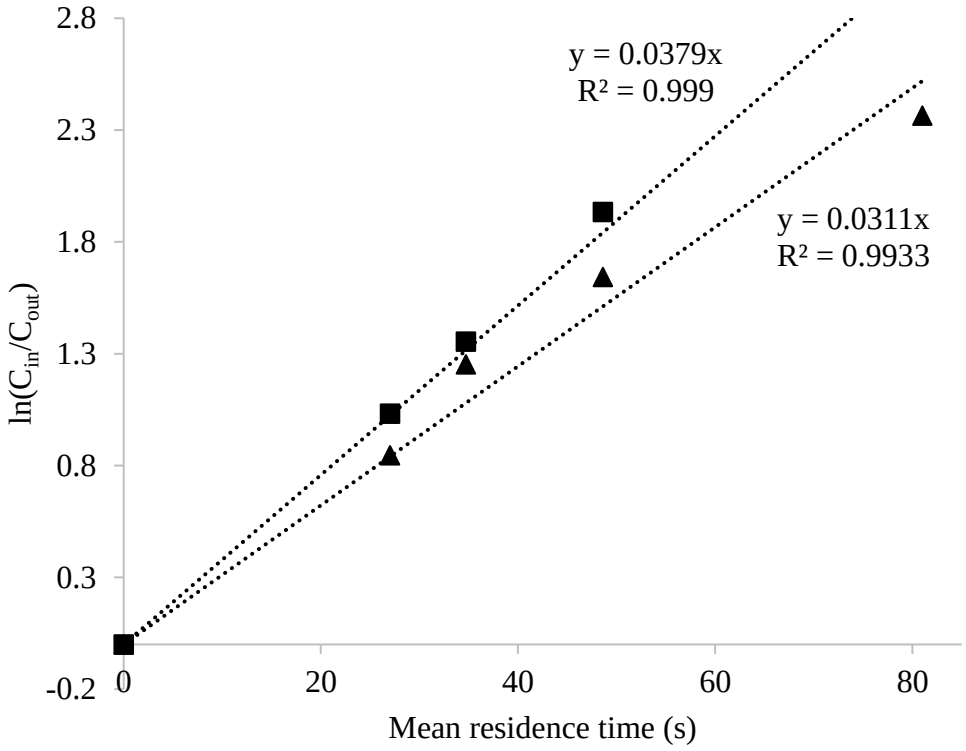


Figure 4.17 Kinetic plot of BPE degradation via EAOP at mean residence times of 27.0, 34.7, 48.6 and 81.0 seconds at fixed current applied of 1.25 mA at varying solvent systems; (■) $MeCN/H_2O$ and (▲) $EtOH/H_2O$

## 4.3 Identification of possible intermediate products and possible reaction pathway mechanism of BPE degradation by EAOP in a microreactor

The intermediate products produced from BPE degradation in both ethanol and acetonitrile co-solvent system are analyzed using Gas Chromatography equipped with a Mass Spectrometry (GC-MS). Nuclear Magnetic Resonance (NMR) have also been used to confirm the presence of aliphatic compounds in the product stream. From the hydrogen peroxide analysis discussed previously, the hydrogen peroxide concentration detected in both ethanol and acetonitrile co-solvent systems are lower than in pure water shown in Figure 4.16. This implies that ethanol and acetonitrile react with hydroxyl radicals producing other compounds or radicals. Therefore, the identification of intermediate products and possible reaction pathway mechanism of BPE degradation by EAOP in a microreactor are split into ethanol/water and acetonitrile/water co-solvent systems.

### 4.3.1 Ethanol/water co-solvent system

The intermediate products shown in Table 4.1 detected by GC-MS are from the degradation of BPE in ethanol/water co-solvent system, carried out by varying flowrate of 3, 5, 7 and 9 ml/h giving a mean residence time of 81.0, 48.6, 34.7 and 27.0 seconds with current fixed at 1.25 mA giving current density of 4.63 $A/m^2$. The intermediate products shown in Table 4.1 are raw data from GC-MS; thus, the actual presence of some of it have not been proven in this research. Normally, in a pure water system, only hydroxyl radicals are being generated via EAOP in the microreactor which plays an important role in the degradation of organic compounds. However, in a co-solvent system, hydroxyl radicals are not the only radicals being generated. For the case of ethanol/water co-solvent system shown in Figure 4.18, ethanol reacts with hydroxyl radicals generating additional radicals namely 1-hydroxyethyl and perhydroxyl radicals [37].

Table 4.1 Intermediate products after degradation of BPE in ethanol/water co-solvent system via EAOP in a microreactor detected from GC-MS

| **Compound** | **Possible compound name** | **Highest 3 Fragments (m/z)** | **Possible Structure** |
|---|---|---|---|
| BPE | Benzyl Phenyl Ether | 184, 91, 65 | 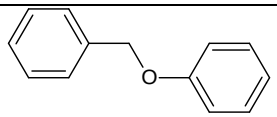 |
| 1 | Benzyl alcohol | 108, 79, 77 | 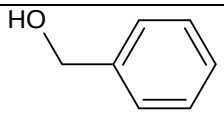 |
| 2 | Benzaldehyde | 106, 77, 51 | 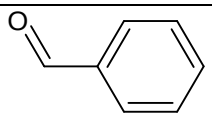 |
| 3 | Benzoic acid | 122, 105, 73 | 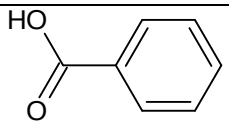 |
| 4 | Benzaldehyde diethylacetal | 135, 107, 73 | 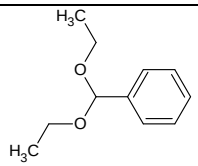 |
| 5 | di-2-phenyl-1,2-propanediol | 105, 73, 44 | 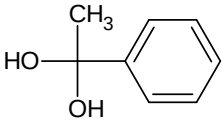 |
| 6 | Benzoic acid, ethyl ester | 121, 105, 73 | 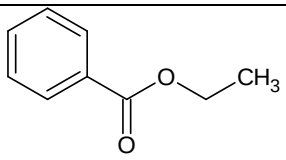 |
| 7 | Phenol, 4-ethoxy- | 138, 110, 73 | 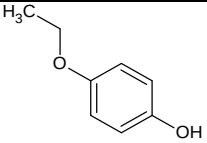 |
| 8 | Nonanal | 73, 57, 44 | 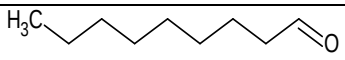 |
| 9 | 2-Butenedioic (Z)-, diethyl ester | 127, 99, 73 | 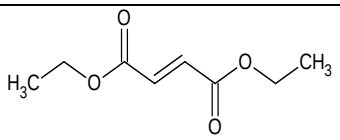 |

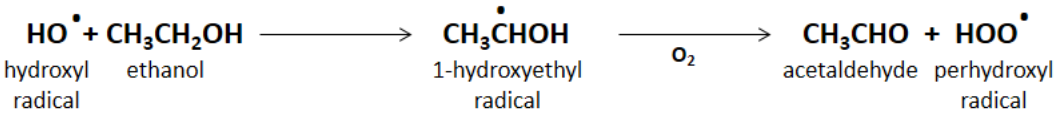


Figure 4.18 Ethanol reaction scheme with hydroxyl radical [37]

A similar α-O-4 lignin model compound called benzyl-O-phenolic (PBP) under similar conditions was reported, reporting 1,4-benzoquinone, benzaldehyde, benzyl alcohol, benzoic acid and hydroquinone as the main products after degradation with Figure 4.19 showing the reaction mechanism [38]. However, only benzaldehyde, benzyl alcohol and benzoic acid have been detected in the product stream shown in Table 4.1. As PBP is quite similar to BPE in structure, the mechanism can be applied to BPE as well with the partial pathway shown in Figure 4.20 showing the pathway from BPE to compound 1, 2 and 3. Compound 4, 5, 6, and 7 are predicted to form from the further reaction between compound 1, 2 and 3 with the free radicals in the system. The free radicals that formed compound 4, 5, 6 and 7 are predicted to be from the free radicals formed from the degradation of ethanol shown in Figure 4.18 as these compounds were not detected from the intermediate products in the degradation of BPE in acetonitrile/water co-solvent system shown in Table 4.2. Therefore, the organic solvent chosen in the co-solvent system will affect the intermediate products formed during degradation as different radicals are formed from the reaction between the organic solvent and hydroxyl radicals.



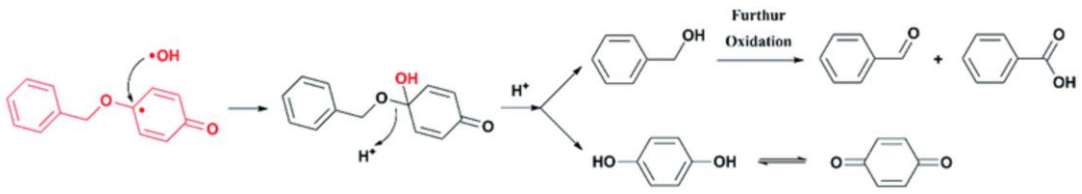


Figure 4.19 PBP (benzyl-O-phenolic) reaction scheme with hydroxyl radical [38]

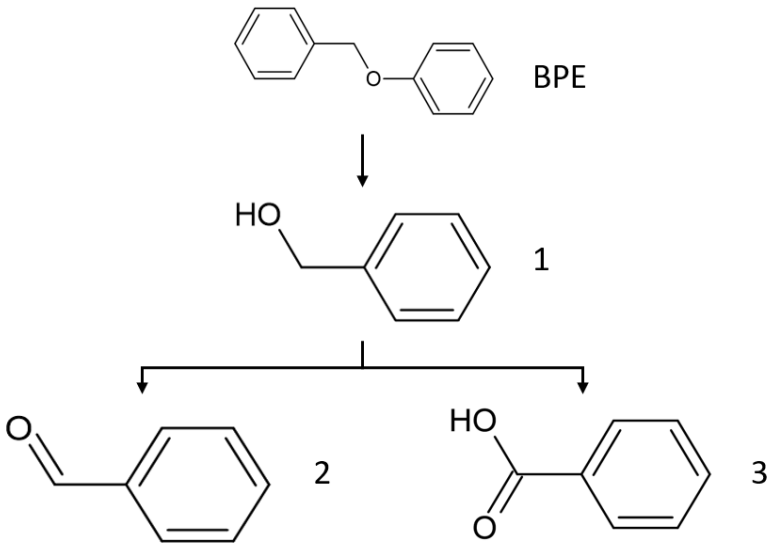


Figure 4.20 Partial reaction pathway of BPE

Compound 8 and 9 are possible aliphatic compounds found in the product stream after degradation of BPE in ethanol/water co-solvent system. The confirmation of the appearance of these aliphatic compounds after degradation can be confirmed using NMR shown in Figure 4.21. Figure 4.21 (a) shows the NMR reading before degradation and Figure 4.21 (b) shows the NMR reading after degradation. The known peaks for ethanol and BPE in Figure 4.21 (a) are identified and labelled [39], [40]. The peaks for ethanol is far stronger when compared to BPE because ethanol is much higher in concentration in the sample at 30 vol% while the concentration of BPE is only 100 mg/L. When comparing both graphs, there is an increase in signal intensity (circled in red) at around 2ppm chemical shift when comparing before and after degradation showing there is an increase in aliphatic compounds after degradation [41]. The formation of these aliphatic compound 8 and 9 are predicted to be formed from the opening of the benzene ring with the mechanism shown in Figure 4.22 [42]–[44]. However, compound 8 and 9 can possibly be formed from the free compounds and radicals in the system especially during the reaction of ethanol with hydroxyl radicals. For this research, the pathway and mechanism of the formation of compound 8 and 9 have not been identified.

Furthermore, the peaks that appear in Figure 4.21 (b) that are not present in Figure 4.21 (a) are assume to be intermediate products formed after the degradation of BPE. However, the peaks circled in orange labelled 1 and 2 in Figure 4.21 (a) are unidentifiable and unknown peaks that are assumed to be contaminants. On the other hand, the signal strength of peak 2 is very strong when compared to the signal strength of both BPE and the aliphatic signal circled in red so it cannot be ignored as just a contaminant signal. However, in this research, the origins or the explanation of peak 2 could not be identified.

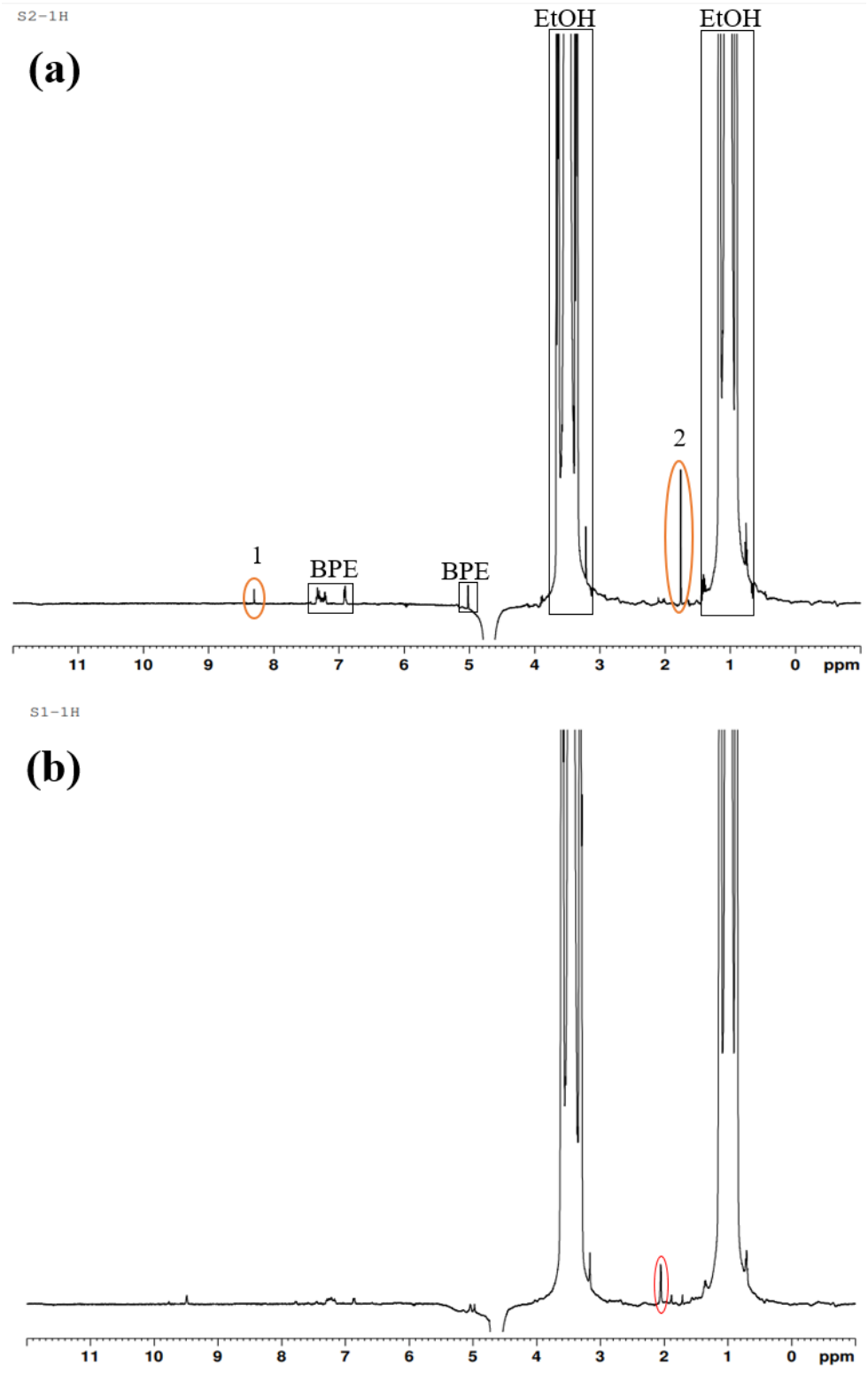


Figure 4.21 NMR results of BPE in ethanol/water co-solvent system; (a) before degradation and (b) after degradation at fixed current of 1.25mA and mean residence time of 27 seconds

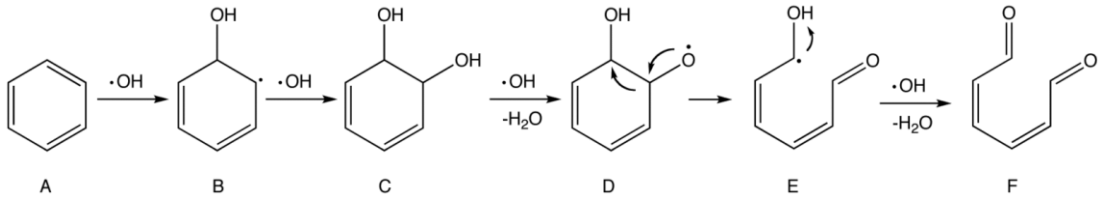


Figure 4.22 Possible benzene ring opening mechanism via oxidation of benzene by hydroxyl radicals [44]

### 4.3.2 Acetonitrile/water co-solvent system

The intermediate products shown in Table 4.2 detected by GC-MS are from the degradation of BPE in acetonitrile/water co-solvent system carried out by varying flowrate of 3, 5, 7 and 9 ml/h giving a mean residence time of 81.0, 48.6, 34.7 and 27.0 seconds with current fixed at 1.25 mA giving current density of 4.63 A/m$^2$. Since the organic solvent in the co-solvent system have been switched to acetonitrile from ethanol, it is expected that the free radicals that are available in the system are different; thus, the detected intermediate products compared are different as well. The intermediate products shown in Table 4.2 are raw data from GC-MS so it has not been confirmed by other methods of analysis. For this research, the reaction pathway and mechanism for the degradation of BPE in acetonitrile/water co-solvent system have not been identified.



Compound 1 and 2 are possible compounds that undergo reaction with free radicals in the system without cleaving the α-O-4 bond in BPE. Next, the formation of compound 3 could possibly be formed from the mechanism discussed before shown in Figure 4.19. Furthermore, benzaldehyde, benzyl alcohol and benzoic acid are predicted to be the first few compounds to form after the cleavage of the α-O-4 bond in BPE in ethanol/water co-solvent system. However, these compounds were not detected in the product stream in acetonitrile/water co-solvent system. This suggests that benzaldehyde, benzyl alcohol and benzoic acid predictably undergo further oxidation with the free radicals in the system to possibly, compound 4, 5, 6, 7, 8, 9

and 10 that have single benzene ring. The additional functional groups present in compound 4, 5, 6, 7, 8, 9 and 10 suggest further reaction of benzaldehyde, benzyl alcohol and benzoic acid with free radicals.

Compound 11 and 12 are possible aliphatic compounds that were detected from GC-MS. The formation of these compounds could possibly from the opening of the benzene ring after further degradation or from the reactions between free radicals in the system. However, the length of compound 11 with 18 carbons is questionable as even if the opening of the benzene ring occurs, it will only provide 6 carbons. Therefore, the actual presence of compound 11 in the product stream is doubtful which requires further investigation to prove its existence.

Table 4.2 Intermediate products after degradation of BPE in acetonitrile/water co-solvent system via EAOP in a microreactor detected from GC-MS

| **Compound** | **Possible compound name** | **Highest 3 Fragments (m/z)** | **Possible Structure** |
|---|---|---|---|
| BPE | Benzyl Phenyl Ether | 184, 91, 65 | 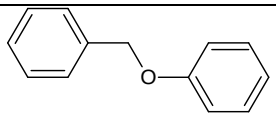 |
| 1 | Benzene, 1,3-dimethyl-2-(phenylmethoxy)- | 207, 91, 44 | 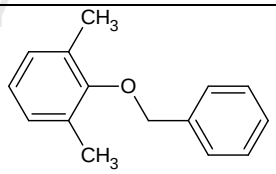 |
| 2 | Benzenepropionic acid, 4-benzyloxy- | 109, 91, 44 | 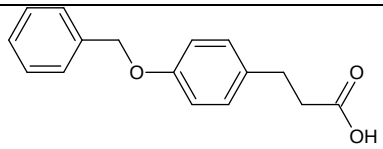 |
| 3 | Hydroquinone | 110, 81, 55 | 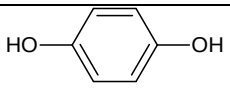 |

| | | | |
|---|---|---|---|
| 4 | 4-Propylbenzaldehyde diethyl acetal | 177, 149, 133 | 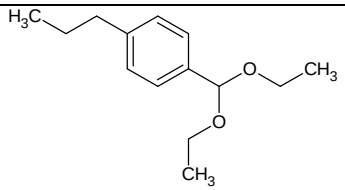 |
| 5 | 4-Ethylbenzoic acid, 2-butyl ester | 177, 151, 133 | 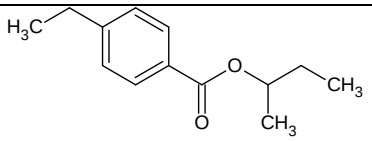 |
| 6 | Benzoic acid, 4-formyl, ethyl ester | 177, 149, 133 | 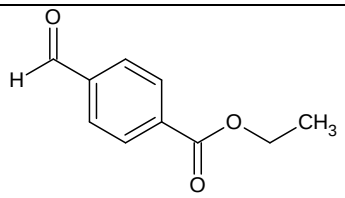 |
| 7 | Diethyl Phthalate | 177, 149, 44 | 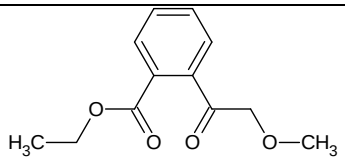 |
| 8 | Acetaminophen | 151, 109, 80 | 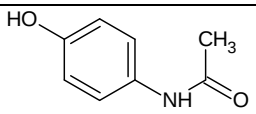 |
| 9 | Dibutyl Phthalate | 223, 149, 44 | 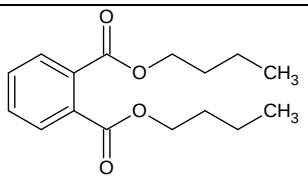 |
| 10 | Acetamide, N-(phenylmethyl)- | 149, 106, 44 | 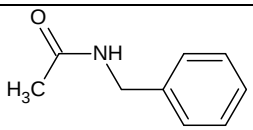 |
| 11 | 9-Octadecenamide, (Z)- | 72, 59, 44 | 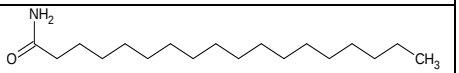 |
| 12 | Triacetin | 145, 103, 43 | 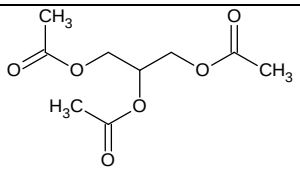 |

# CHAPTER 5

# CONCLUSION

This chapter concludes this research in 3 section which are the summary of results, conclusion and recommendations.

## 5.1 Summary of results

1. Benzyl phenyl ether (BPE) was used as the lignin model compound to mimic the α-O-4 bond.
2. The co-solvent with 30 vol% organic solvent is most optimum to use in the degradation of BPE.
3. Benzyl phenyl ether can be degraded by the generation of hydroxyl radicals ($OH^*$) from water in the co-solvent via electrochemical oxidation process (EAOP).
4. The hydroxyl radicals can be quantified by measuring the concentration of hydrogen peroxide in the system.
5. The variation of mean residence time, applied current, concentration of solvent and type of solvent affects the degradation of BPE and generation of hydroxyl radicals.
6. The degradation of BPE follows the pseudo-first order reaction even with the variation of mean residence time, applied current, concentration of solvent and type of solvent.
7. Kinetics in the reactor of the system dominates transport phenomena.

8. The type of organic solvent in the co-solvent system affects the intermediate products being formed.
9. Long aliphatic carbon chains are detected in the product stream after degradation.

## 5.2 Conclusion

The degradation of benzyl phenyl ether (BPE) was successfully degraded via electrochemical advanced oxidation process (EAOP) in a microreactor through the generation of hydroxyl radicals from water. 30 vol% of organic solvent in the co-solvent system provided the system a balance of both solubility and conversion. The degradation of BPE depends on the formation of hydroxyl radicals which can be quantify by measuring the concentration of hydrogen peroxide in the system. The parameters that give the highest degradation of BPE and highest concentration of hydrogen peroxide are mean residence time of 81.0 seconds, applied current of 8.33 $A/m^2$ and 30% vol acetonitrile/water co-solvent system. The increase in mean residence time and applied current increases the degradation of BPE which is consistent with the increase of the concentration of hydrogen peroxide. Ethanol through literature, is a much stronger hydroxyl radical scavenger than acetonitrile but only observe a slight increase in degradation of BPE in acetonitrile co-solvent system. The intermediate products detected after the degradation of BPE was also discussed where different products were observed for ethanol/water and acetonitrile/water co-solvent system due to both producing different radicals when the organic solvent reacts with hydroxyl radicals. Partial reaction pathway and partial mechanisms were also discussed.

## 5.3 Recommendations

The potential research work that can be further investigated on in the future for the degradation of BPE via EAOP in a microreactor include:

1. The study of other lignin bonds such as β-O-4, β−β and β-5 bonds.
2. The effect of temperature of the degradation of BPE and intermediates formed.
3. Quantification of the intermediates after the degradation of BPE.
4. Investigation of the complete pathway and mechanism for ethanol/water and acetonitrile/water co-solvent system after the degradation of BPE.

The parameters that are found to be crucial in this research that need to be considered if this technology were to be commercialized in the future assuming that the commercial lignin used is insoluble in water are the mean residence time, applied current, concentration of organic solvent and type of organic solvent. All these parameters are important parameters to be optimized as every parameter will affect the feasibility of commercialization. The unique parameter that was studied in this research is the organic solvent which affects the degradation performance as the organic solvent will take up some of the hydroxyl radicals producing its own radicals which will then produce different products. As for scaling up, the parameters that need to be considered include the expected output, the expected degradation efficiency, size of the microreactor and cost. The expected output and degradation efficiency will determine the size of the microreactor but if the expected output is too much for one microreactor to handle then multiple microreactors can be considered as well. The recuring cost which excludes the initial cost to build and install the microreactor that need to be considered for it to be commercially feasible include the cost of electricity and cost of replacing the graphite anode. However, before scaling up, the challenge of separating the products after degradation need to be investigated for it to be commercially feasible.

# REFERENCES


[1] "bp Statistical Review of World Energy 2020," p. 68, 2020.

[2] H. Ritchie and M. Roser, "Fossil Fuels," *Our World Data*, Oct. 2017, Accessed: Jun. 26, 2021. [Online]. Available: https://ourworldindata.org/fossil-fuels

[3] T. K. F. Dier, D. Rauber, D. Durneata, R. Hempelmann, and D. A. Volmer, "Sustainable Electrochemical Depolymerization of Lignin in Reusable Ionic Liquids," *Sci. Rep.*, vol. 7, no. 1, p. 5041, Jul. 2017, doi: 10.1038/s41598-017-05316-x.

[4] K. Yan, Y. Zhang, M. Tu, and Y. Sun, "Electrocatalytic Valorization of Organosolv Lignin Utilizing a Nickel-Based Electrocatalyst," *Energy Fuels*, vol. 34, no. 10, pp. 12703–12709, Oct. 2020, doi: 10.1021/acs.energyfuels.0c02284.

[5] H. Y. Lim *et al.*, "Review on Conversion of Lignin Waste into Value-Added Resources in Tropical Countries," *Waste Biomass Valorization*, vol. 12, no. 10, pp. 5285–5302, Oct. 2021, doi: 10.1007/s12649-020-01307-8.

[6] C. Ververis, K. Georghiou, N. Christodoulakis, P. Santas, and R. Santas, "Fiber dimensions, lignin and cellulose content of various plant materials and their suitability for paper production," *Ind. Crops Prod.*, vol. 19, no. 3, pp. 245–254, May 2004, doi: 10.1016/j.indcrop.2003.10.006.

[7] O. Y. Abdelaziz *et al.*, "Biological valorization of low molecular weight lignin," *Biotechnol. Adv.*, vol. 34, no. 8, pp. 1318–1346, Dec. 2016, doi: 10.1016/j.biotechadv.2016.10.001.

[8] R. Xu *et al.*, "Lignin depolymerization and utilization by bacteria," *Bioresour. Technol.*, vol. 269, pp. 557–566, Dec. 2018, doi: 10.1016/j.biortech.2018.08.118.

[9] E. Jasiukaitytė-Grojzdek, M. Huš, M. Grilc, and B. Likozar, "Acid-catalysed α-O-4 aryl-ether bond cleavage in methanol/(aqueous) ethanol: understanding depolymerisation of a lignin model compound during organosolv pretreatment," *Sci. Rep.*, vol. 10, no. 1, p. 11037, Jul. 2020, doi: 10.1038/s41598-020-67787-9.

[10] A. Kumar, Anushree, J. Kumar, and T. Bhaskar, "Utilization of lignin: A sustainable and eco-friendly approach," *J. Energy Inst.*, vol. 93, no. 1, pp. 235–271, Feb. 2020, doi: 10.1016/j.joei.2019.03.005.

[11] B. MAHDAVI, A. LAFRANCE, A. MARTEL, J. LESSARD, H. ME´NARD, and L. BROSSARD, "Electrocatalytic hydrogenolysis of lignin model dimers at Raney nickel electrodes," *J. Appl. Electrochem.*, vol. 27, no. 5, pp. 605–611, May 1997, doi: 10.1023/A:1018463131891.

[12] B. Matsagar *et al.*, "Efficient Liquid-Phase Hydrogenolysis of Lignin Model Compound (Benzyl Phenyl Ether) Using a Ni/Carbon Catalyst," *React. Chem. Eng.*, vol. 4, Jan. 2019, doi: 10.1039/C8RE00304A.

[13] X. Du, H. Zhang, K. P. Sullivan, P. Gogoi, and Y. Deng, "Electrochemical Lignin Conversion," *ChemSusChem*, vol. 13, no. 17, pp. 4318–4343, 2020, doi: https://doi.org/10.1002/cssc.202001187.

[14] F. Streffer, "Lignocellulose to Biogas and other Products," *JSM Biotechnol Bioeng*, vol. 2, p. 1023, May 2014.

[15] V. Menon and M. Rao, "Trends in bioconversion of lignocellulose: Biofuels, platform chemicals & biorefinery concept," *Prog. Energy Combust. Sci.*, vol. 38, no. 4, pp. 522–550, Aug. 2012, doi: 10.1016/j.pecs.2012.02.002.

[16] W. Boerjan, J. Ralph, and M. Baucher, "Lignin Biosynthesis," *Annu. Rev. Plant*

*Biol.*, vol. 54, pp. 519–46, Feb. 2003, doi: 10.1146/annurev.arplant.54.031902.134938.

[17] S. Laurichesse and L. Avérous, "Chemical modification of lignins: Towards biobased polymers," *Top. Issue Biomater.*, vol. 39, no. 7, pp. 1266–1290, Jul. 2014, doi: 10.1016/j.progpolymsci.2013.11.004.

[18] C. W. Lahive, P. C. J. Kamer, C. S. Lancefield, and P. J. Deuss, "An Introduction to Model Compounds of Lignin Linking Motifs; Synthesis and Selection Considerations for Reactivity Studies," *ChemSusChem*, vol. 13, no. 17, pp. 4238–4265, Sep. 2020, doi: 10.1002/cssc.202000989.

[19] C. li, X. Zhao, A. Wang, G. Huber, and T. Zhang, "Catalytic Transformation of Lignin for the Production of Chemicals and Fuels," *Chem. Rev.*, vol. 115, Oct. 2015, doi: 10.1021/acs.chemrev.5b00155.

[20] G. Vázquez, G. Antorrena, J. González, and S. Freire, "The Influence of Pulping Conditions on the Structure of Acetosolv Eucalyptus Lignins," *J. Wood Chem. Technol.*, vol. 17, no. 1–2, pp. 147–162, Feb. 1997, doi: 10.1080/02773819708003124.

[21] S. Baumberger *et al.*, "Molar mass determination of lignins by size-exclusion chromatography: towards standardisation of the method," vol. 61, no. 4, pp. 459–468, 2007, doi: 10.1515/HF.2007.074.

[22] A. Vishtal and A. Kraslawski, "Challenges in industrial applications of technical lignins," *Bioresources*, vol. 6, pp. 3547–3568, Jun. 2011, doi: 10.15376/biores.6.3.3547-3568.

[23] P. Sannigrahi, A. J. Ragauskas, and S. J. Miller, "Lignin Structural Modifications Resulting from Ethanol Organosolv Treatment of Loblolly Pine," *Energy Fuels*, vol. 24, no. 1, pp. 683–689, Jan. 2010, doi: 10.1021/ef900845t.

[24] J. Chen, H. Yang, H.-Q. Fu, H. He, Q. Zeng, and X. Li, "Electrochemical oxidation mechanisms for selective products from C−O and C−C cleavages of a β−O−4 linkage in lignin model compounds," *Phys. Chem. Chem. Phys.*, vol. 22, Apr. 2020, doi: 10.1039/D0CP01091J.

[25] B. Güvenatam, O. Kurşun, E. H. J. Heeres, E. A. Pidko, and E. J. M. Hensen, "Hydrodeoxygenation of mono- and dimeric lignin model compounds on noble metal catalysts," *Catal. Mater. Catal. Low Carbon Technol.*, vol. 233, pp. 83–91, Sep. 2014, doi: 10.1016/j.cattod.2013.12.011.

[26] I. Sirés, E. Brillas, M. A. Oturan, M. A. Rodrigo, and M. Panizza, "Electrochemical advanced oxidation processes: today and tomorrow. A review," *Environ. Sci. Pollut. Res.*, vol. 21, no. 14, pp. 8336–8367, Jul. 2014, doi: 10.1007/s11356-014-2783-1.

[27] M. Fryda, T. Matthée, S. Mulcahy, M. Höfer, L. Schäfer, and I. Tröster, "Applications of DIACHEM ® Electrodes in Electrolytic Water Treatment," *Electrochem. Soc. Interface*, vol. 12, pp. 40–44, Mar. 2003, doi: 10.1149/2.F10031IF.

[28] C. Fang, M. Megharaj, and R. Naidu, "Electrochemical Advanced Oxidation Processes (EAOP) to degrade per- and polyfluoroalkyl substances (PFASs)," *J. Adv. Oxid. Technol.*, vol. 20, no. 2, 2017, doi: 10.1515/jaots-2017-0014.

[29] W. Khongthon, "Degradation of diuron via an electrochemical advanced oxidation process in a microscale-based reactor," 2015.

[30] "Benzyl phenyl ether, 97%, Thermo Scientific | Fisher Scientific."

https://www.fishersci.com/shop/products/benzyl-phenyl-ether-97-thermo-scientific/AAB2253906 (accessed Oct. 21, 2021).

[31] P.-A. Michaud, M. Panizza, L. Ouattara, T. Diaco, G. Foti, and Ch. Comninellis, "Electrochemical oxidation of water on synthetic boron-doped diamond thin film anodes," *J. Appl. Electrochem.*, vol. 33, no. 2, pp. 151–154, Feb. 2003, doi: 10.1023/A:1024084924058.

[32] A. Kapalka, G. Foti, and C. Comninellis, "The importance of electrode material in environmental electrochemistry: Formation and reactivity of free hydroxyl radicals on boron-doped diamond electrodes," *Electrochimica Acta*, vol. 54, pp. 2018–2023, Feb. 2009, doi: 10.1016/j.electacta.2008.06.045.

[33] Y. Cao, C. Soares, N. Padoin, and T. Noel, "Gas Bubbles Have Controversial Effects on Taylor Flow Electrochemistry," *Chem. Eng. J.*, vol. 406, p. 126811, Sep. 2020, doi: 10.1016/j.cej.2020.126811.

[34] R. Parthasarathi, R. A. Romero, A. Redondo, and S. Gnanakaran, "Theoretical Study of the Remarkably Diverse Linkages in Lignin," *J. Phys. Chem. Lett.*, vol. 2, no. 20, pp. 2660–2666, Oct. 2011, doi: 10.1021/jz201201q.

[35] V. Múčka, P. Bláha, V. Čuba, and J. Červenák, "Influence of various scavengers of •OH radicals on the radiation sensitivity of yeast and bacteria," *Int. J. Radiat. Biol.*, vol. 89, no. 12, pp. 1045–1052, Dec. 2013, doi: 10.3109/09553002.2013.817702.

[36] X. Li, "Solvent effects and improvements in the deoxyribose degradation assay for hydroxyl radical-scavenging," *Food Chem.*, vol. 141, no. 3, pp. 2083–2088, Dec. 2013, doi: 10.1016/j.foodchem.2013.05.084.

[37] D. De Schutter, D. Saison, D. F., G. Derdelinckx, and F. Delvaux, "The chemistry of aging beer," in *Beer in Health and Disease Prevention*, 2009, pp. 375-388 (vol.1).

[38] L. Wang *et al.*, "Study on the cleavage of alkyl-O-aryl bonds by in situ generated hydroxyl radicals on an ORR cathode," *RSC Adv.*, vol. 7, no. 81, pp. 51419–51425, 2017, doi: 10.1039/C7RA11236J.

[39] I. Gerothanassis, A. Troganis, V. Exarchou, and K. BARBAROSSOU, "Nuclear magnetic resonance (NMR) spectroscopy: Basic principles and phenomena, and their applications to chemistry, biology and medicine," *Chem Educ Res Pr.*, vol. 3, May 2002, doi: 10.1039/B2RP90018A.

[40] "BENZYL PHENYL ETHER(946-80-5) 13C NMR spectrum." https://www.chemicalbook.com/SpectrumEN_946-80-5_13CNMR.htm (accessed Jun. 21, 2022).

[41] S. Wolfrum *et al.*, "Utilization of Sc3N@C-80 in long-range charge transfer reactions," *Chem. Commun. Camb. Engl.*, vol. 47, pp. 2270–2, Feb. 2011, doi: 10.1039/c0cc04159a.

[42] X.-M. Pan, M. N. Schuchmann, and C. von Sonntag, "Oxidation of benzene by the OH radical. A product and pulse radiolysis study in oxygenated aqueous solution," *J. Chem. Soc. Perkin Trans. 2*, no. 3, pp. 289–297, 1993, doi: 10.1039/P29930000289.

[43] R. Watts and A. Teel, "Chemistry of Modified Fenton's Reagent (Catalyzed H2 O2 Propagations–CHP) for In Situ Soil and Groundwater Remediation," *J. Environ. Eng.-Asce - J Env. ENG-ASCE*, vol. 131, Apr. 2005, doi: 10.1061/(ASCE)0733-9372(2005)131:4(612).

[44] Solarchem Environmental Systems., *The UV/oxidation handbook.* Markham, Ont., Canada; Las Vegas, Nev.: Solarchem Environmental Systems, 1994.

# VITA

| | |
|---|---|
| **NAME** | Lee Kevin |
| **DATE OF BIRTH** | 23 July 1997 |
| **PLACE OF BIRTH** | Klang, Selangor, Malaysia |